INSTITUTO SUPERIOR DE CIÊNCIAS DA SAÚDE EGAS MONIZ

ERASMUS MUNDUS MASTER IN FORENSIC SCIENCE

THE USE OF WAVELENGTH-DISPERSIVE X-RAY FLUORESCENCE (WDXRF) SPECTROSCOPY AND MULTIVARIATE TECHNIQUES FOR THE ASSESSMENT OF ILLEGAL DYES IN SPICES

Work submitted by

Emmanuel Adusei

for Master's Degree in Forensic Science

Supervised by

Prof. Dra. Luisa Gonçalves

JULY 2014

Certificate of Originality

This is to certify that I am responsible for the work submitted in this thesis and that the work is original and not copied or plagiarised from any other source, except as specified in the acknowledgements and in references. Neither the thesis nor the original work contained therein has been submitted to any institution for a degree.

Signature: 

Name: Emmanuel Adusei

Date: 9th July, 2014

Dedication

This work is dedicated to God Almighty who gave me the life and strength for this work, to my Father-in-law Pastor Emmanuel Abbey and my sister Gloria Nyarkoa-Adusei, who didn't live to see this season in my life.

Acknowledgement

To Dra. Luisa Gonçalves my supervisor, you have been so instrumental in the success of this work. Prof. Jose Brito, your expertise in XRF and statistics made this work a success. I thank you both for your advices, constructive criticisms, and suggestions for making this work a success. I could not have made it without you.
Tania Fernandez, thank your for all the sacrifices you made in this project.
To all tutors in this Erasmus Mundus course, who taught me one thing or the other, and showed great professionalism and friendship, I say thank you all.
I also appreciate the support and encouragement from my wife Mrs Eunice Adusei who has been a wonderful companion throughout this whole Master's course.
Finally, I thank the European Commission for the financial support for the study and the entire Erasmus Mundus Masters in Forensic Science Program. This had made my dream of becoming a Forensic Scientist a reality.

Abstract:

Sudan dyes are synthetic azo and diazo compounds that are banned for use in food worldwide including the European Community due to their potential toxicity to humans. The ability of WDXRF spectroscopic technique to predict the levels of adulteration of paprika and sweet pepper suspected to be adulterated with Sudan I-IV, Para Red and Sunset Yellow FCF dyes was investigated in this study. Logistic regression and discriminant analysis classification models were developed to predict the type of adulteration using WDXRF spectral features such as the Compton and Rayleigh scatter intensities and the Compton and Rayleigh ratios. Prediction of the levels of adulteration was assessed by using multiple regression analysis. 83% of the 210 adulterated samples were correctly classified by the logistic regression with 90% sensitivity, 75%specificity with a prediction power of 92% into respective adulteration groups. 86% and 90% correct prediction were obtained for discriminant analysis models with 94% sensitivity and 74% specificity. Three multiple regression models were performed for each data set. Models based on the Compton and Rayleigh ratios, Compton and Rayleigh scatter intensities as well as a full model based on both ratios and scatter intensities were developed and compared with each other. The full model revealed to be the best model to predict the levels of adulteration with an adjusted R^2 between 95.1 to 99.0% with the errors of estimate between 1.6 to 3.7%.

To the best of the author's knowledge, this is the first time such methodological approach was used for the purposes of screening illegal dyes in food matrices. Moreover, WDXRF technique may represent a promising tool for the screening of Sudan dyes-adulterated spices and can be used as an alternative to classical methods for determining Sudan dyes present in food.

Keywords: Spices, Sudan dyes, WDXRF, multiple regression, logistic regression

List of Figures

List of Tables

List of Abbreviations

ASTA: American Spice Trade Association

CAS: Chemical Abstracts Service

CI: Colour Index

DA: Discriminant Analysis

EFSA: European Food Safety Authority

ELISA: Enzyme-Linked Immunosorbent Assay

ESI: Electron Spray Ionisation

EU/EC: European Union / European Community

FSA: Food Standards Authority

FSS: Food Safety and Standards

FTIR: Fourier Transformed Infra-Red

GIT: Gastrointestinal Tract

^{1}HNMR: Proton Nuclear Magnetic Resonance

HPLC: High Performance Liquid Chromatography

IARC: International Agency for Research in Cancer

IUPAC: International Union of Pure and Applied Chemistry

LOD: Limit of Detection

MS: Mass Spectrometer

NIR: Near Infra-Red

PLS-DA: Partial Least Squares – Discriminant Analysis

RASFF: Rapid Alert System for Food and Feed

RPLC: Reverse Phase Liquid Chromatography

SERS: Surface-Enhanced Raman Spectroscopy

SY: Sunset Yellow FCF dye

UPLC: Ultra-high Performance Liquid Chromatography

WDXRF: Wavelength-Dispersive X-Ray Fluorescence

XRF: X-Ray Fluorescence

Table of Contents

1. INTRODUCTION

1.0 Background

Food quality is closely related to its colour and the use of colorants has been an age-old practice to enhance the aesthetic appeal of foods (Downham & Collins, 2000). Food adulteration is achieved by the addition, substitution or removal of ingredients from food. Due to the lack of stability of natural colorants under some food processing and/or conditions, other colorants are used. Synthetic dyes or colorants are recognised as the most reliable and economical for restoring or providing colour to processed food products. Azo dyes are the most widely used synthetic dyes for wide applications including industrial and scientific applications. They constitute about 70% of organic colorants produced worldwide with respect to the number and production volume (Bafana et al., 2011).

Sudan dyes (Sudan I-IV, Sudan Red, Red 7B, Red G, Orange G, Sudan Black, Para Red, Dimethyl Yellow, Toluidine Red and Orange II) are a class of azo dyes with wide range of industrial and scientific applications such as coloring of plastics, waxes, textiles, fuels, and staining for microscopy. Besides, Sudan dyes have been used in foodstuffs such as culinary spices to maintain their colours for commercial benefits due to their low cost, bright colours, long maintenance and wide availability. However, Sudan dyes have been classified as category 3 carcinogens (IARC, 1975) because of the potential conversion of their metabolites to active carcinogens and mutagens in humans (Fonovich, 2013; Pan et al., 2012). Sunset Yellow FCF (SY) is an azo dye that is allowed as a food additive in the European Union (EU) and several countries worldwide (EFSA Scientific Opinion 2009; Yadav et al., 2013). It is used in food preparations such as confectionary products, candies, sweets, frozen desserts and beverages, cosmetics, medicines and dietary supplements (Dixit et al., 2008, 2011; Tripathi et al., 2010; Yadav et al., 2013; Tripathi et al., 2007, Rao and Sudershan, 2008). However, with a maximum permitted level of SY in food commodities being 100-200 parts per million (ppm), studies have reported that the limit is usually exceeded in manifolds (Dixit et al., 2008; Tripathi *et al* 2007). Additionally, SY have been found to be present in food commodities such as tomato sauce in which the use of SY as colorant is prohibited (Dixit et al., 2008).

1.1 What are Dyes or Colorants?

Dyes can be defined as substances which, when applied to a substrate, impart colour to a substrate. The adherence of dyes onto the surfaces of substrates are made by processes such as physical adsorption, mechanical retention, chemical reaction with formation of covalent bonds or complexes with salts or metals via solubilization (Kirk-Othmer 2004). The colour of a particular dye depends on its ability to absorb light in the visible range of the electromagnetic spectrum (400-700nm). According to the Witt theory, a coloured dye is composed of a chromophore group and an auxochrome group. Chromophores impart colour to the dye because of their capability of absorbing light in the visible region (e.g., azo, nitro, and quinoid groups), while auxochromes deepen the colour when introduced into a coloured molecule. The Witt theory has been replaced by a theory (Bafana et al., 2011) which states that colour is caused by the excitation of valence π electrons by visible light (Murrell, 1973).

1.2 Types of Dyes

1.2.1 Natural and 'Nature-identical' colorants or dyes

Natural dyes were the first to be used by humans. Most of the natural dyes were extracts from vegetables and a few from animal products. However, the ranges of colours were as limited as were the utility of the dyes. Until the 19th century, all dyes were from natural sources. Due to the limited range and instability of natural dyes (sensitive to pH, light, oxidation, etc.) as at then, chemists synthesized new dyes and consequently new colours; with the introduction of synthetic dyes, the use of natural dyes has almost been discontinued (Garfield 2002). However, with the growing concerns of health regarding the use of synthetic dyes, there has been the increased production of natural dyes in the past 25 years and 'nature-identical' colours. Natural colours that are present in food include lycopene, lutein, curcumin, bixin/nobixin, capsanthin/capsorubin, chlorophyll, carmin and carminic acid, etc. The 'nature-identical' were synthesized to match their natural counterparts. The most synthesized nature-identical pigments are the carotenoids, but they are prone to oxidation and subsequent loss of colour (Downham & Collins, 2000).

1.2.2 Synthetic Dyes

Synthetic dyes which were first produced were based mainly on aniline, which was obtained from coal-tar, hence the name "coal-tar dyes". Chemically, dyes can be inorganic or organic compounds. Based on their chemical composition and application class, synthetic dyes are divided into acid, azoic, basic, direct, disperse, mordant, reactive, sulphur, and vat dyes. Alternatively, synthetic dyes can be chemically divided into azo, nitro, nitrosso, xanthene, etc. Synthetic dyes or colorants are recognised as the most reliable and economical for restoring or providing colour to processed food products (Downham & Collins, 2000).

1.2.3 Azo dyes

Azo dyes are synthetic compounds bearing the functional group R_1-N=N=R_2, where R_1 and R_2 are alkyl and/or aryl substituents. According to Figure 1, these compounds are characterized by having one or two azo bonds (Chung et al., 1992; Collier et al., 1993; Rafii et al., 1997).They constitute about 60-70% of the organic dyes that are produced worldwide, with respect to number and production volume (Bafana et al., 2011). At least, about 3,000 of azo dye are used extensively as colorants in food, cosmetics, textiles, pharmaceutical products, paper, etc. Some are also used for scientific purposes such as in microscopic stains (Downham & Collins, 2000). The first azo dyes to be manufactured were Aniline Yellow and Bismark Brown by Mene in 1861 and by Martius in 1863, respectively. However, the first azo dye produced from diazotization and azo coupling, as utilized in modern industry, was performed in 1875 by Caro and Witt at BASF (Badische Anilin & Soda-Fabrik), Germany (Bafana et al., 2011; Downham & Collins, 2000). Examples of azo dyes are Sudan dyes (Sudan I, II, III, IV, and Para Red), Sunset Yellow FCF, Tatrazine, Orange I and II, etc.

A single dye could have many different names. For example, Rose Red dye has three names; Rosaniline, Magenta, and Fuchsine. To avoid this difficulty, the Society of Dyers and Colourists, and the American Association of Textile Chemists and Colourists compiled a Colour Index (CI) in which each dye is given a CI number (Colour Index 2001). Azo dyes or colorants are rarely referred by IUPAC (International Union of Pure and Applied Chemistry) or CAS (Chemical Abstracts Service) nomenclature due to the complexity of their chemical names (Bafana et al., 2011). In the CI system, azo dyes are provided with numbers ranging from 11000 to

39999 which corresponds to their chemical classes. Figure 1 presents the chemical structures of Sudan dyes, their respective CAS numbers (in between brackets) and systematic name.

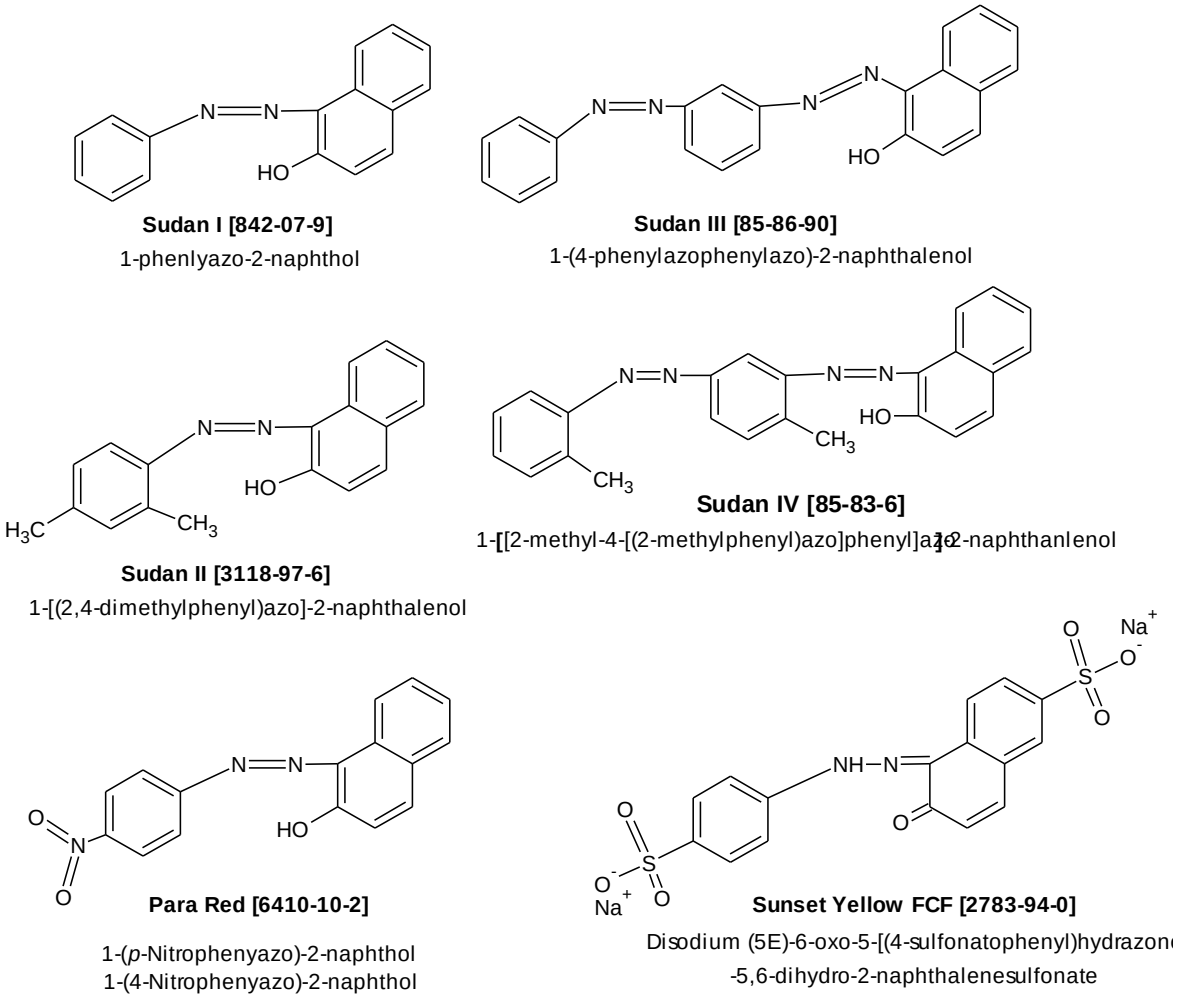

Figure 1: Chemical structures of the azo dyes discussed in this work

.

1.3 Trends in adulteration of food with Sudan dyes

Sudan I was first detected in ground capsicum imported from India into the European Community in May 2003. The European Authority reported levels of adulteration of 4,000ppm found the capsicum imported by shippers from Mumbai (ASTA, 2005). In response to the adulteration, the European Union implemented Decision 2003/460/EC as a condition for which all imported hot chilli and chilli products were screened for Sudan I. The Decision was later amended in 2004 (Commission Decision 2004/92/EC) to include screening for Sudan II, III, and IV dyes as well. In 2004, Sudan dyes were

detected in unrefined palm oil imported into the EU. Commission Decision (2005) was implemented which required the certification of all chilli-, curry-, and curcuma-containing food and palm oil imported into the Community to be free of Sudan dyes. In 2005, the UK Food Standards Agency (FSA) reported of the detection of Sudan I in Worcester sauce produced in the UK and leading to the recall of food products containing the sauce. Investigations revealed that the source of the dye was contaminated chilli imported into the UK in 2002 prior to the implementation of Commission Decision 2003/460/EC. Other recalls ensued in countries like Canada, China and South Africa. In April and May 2005, products contaminated with Para Red were recalled in the UK (ASTA, 2005). Recently, in 2014, the Indian Spices Board ordered exporters to destroy all consignments of spices which were found to be contaminated with Sudan dyes, in compliance with FSS Act 2006 (foodsafetyhelpline.com).

Apart from the health hazards imposed by consumption of these carcinogenic Sudan dyes, there are other very costly implications for companies involved in the adulteration and others as well. For example, it was estimated that in the EU alone, Sudan dyes-related problems had cost hundreds of millions of dollars. The costs of recalling of adulterated food products are very huge with numerous companies bearing the financial burden of testing. Honest suppliers from India who supplied Sudan-free spices had also lost their businesses since buyers sourced other markets (ASTA, 2005).

1.4 Nature, Metabolism and Toxicity of the azo dyes

Under anaerobic conditions, azo dyes can be reduced by azoreductase to colourless amines via reduction of the azo bonds as the first step of their metabolism (Chen et al., 2005, 2010; Feng et al., 2010). It is known that the reduction of the azo bonds to the above-mentioned compounds is accountable for the toxicity, mutagenicity and carcinogenicity associated with azo dyes (Chen 2006). The microflora of the human skin and gastrointestinal tract (GIT) have both been reported to metabolize Sudan dyes, leading to the generation of ranges of carcinogenic amines, such as aniline and methylanilines, naphthylamines, etc. (Fonovich, 2013).

1.4.1 Sudan I

Sudan I (C.I. Solvent Yellow 14), is a monoazo dye with the chemical formula 1-phenylazo-2-naphthol (Figure 1). Theoretically, Sudan I is reduced to predominantly aniline and 1-amino-2-naphthol (Pan et al., 2012). Stiborova et al. (2002) first reported the metabolism of Sudan I by human cytochrome P450s (CYPs) in liver microsomes with a pattern similar to the reduction of Sudan I by rat CYPs responsible for carcinogenicity in the animal. They also found that Sudan I was best metabolized by rat CYP1A1 and recombinant human CYP1A1 (Stiborová et al., 2002, 2005). Recent studies showed that Sudan I induced CYP 1A1 and NAD(P)H: quinone oxidoreductase 1 (NQO1) in rat liver, kidneys and lungs (Stiborová et al., 2013). Besides, Sudan I showed genotoxic effects in HepG2 cells (An et al., 2007) and increased mutagenic and clastogenic effects in MCL-5 cell lines (Johnson et al., 2010). Stiborova et al. (2006) detected Sudan I-DNA adducts in the rat liver which suggested the possible carcinogenic mechanism of Sudan I in the liver, mediated by CYP1A1-mediated oxidative reactions by cytochrome b_5 (Fonovich 2013; Stiborova et al., 2006). Sudan I was reported to give positive results for Salmonella typhimurium mutagenicity test in rat liver with S9 activation (Ames test) (Zeiger et al., 1988). Recently, Xu et al. (2007), after anaerobic incubation of Sudan dyes with fresh dilutions of human faecal suspensions, reported that Sudan I was completely metabolized within 24-30 hours by the human gastrointestinal bacteria predominately to aniline (Xu et al., 2007, 2010).

1.4.2 Sudan II

Sudan II (C.I. Solvent Orange 7) is a dimethyl derivative of Sudan I (Figure 1) with the chemical formula (1-[(2,4-dimethylphenyl)azo]-2-naphthalenol. Early studies showed Sudan II to induce mutation of Salmonella typhimurium TA 1538 in the presence of rat liver, and gave positive results with standard plate-incorporation and FMN pre-incubation modification of Salmonella assays (Garner and Nutman, 1977; Cameron et al., 1987). Similarly to Sudan I, Sudan II was metabolized predominately to 2,4-dimethylaniline in addition to 1-amino-2-naphthol and was also degraded to dimethylaniline within 24-30 hours following anaerobic incubation with fresh human faecal suspension. Besides, it was reported that 2,4-dimethlylaniline metabolite of Sudan II induced DNA damage mice liver cells when tested with the comet assay under alkaline conditions (Xu et al., 2010). Further, Xu et al. (2010) studied the

capacity of 35 prevalent human intestinal bacterial species to degrade Sudan dyes and Para Red. The study concluded that, with the exception of Sudan II, the bacterial species in the human colon easily degraded Sudan and Para Red dyes to their respective aromatic amine metabolites.

1.4.3 Sudan III, IV and Para Red

Sudan III (C.I. Solvent Red 23) or 1-[4-(phenylazo)phenylazo]-2-naphthol is approved for use in drugs and cosmetics. It is predominately degraded into 1,4-phenylenediamine and aniline, in addition to 1-amino-2-naphthol. Sudan III was reported to have increased the breaks in metaphase stage, during an *in vitro* investigation of clastogenic potential of Sudan III with hamster ovary cells (CHO) without metabolic activation (Au and Hsu, 1979). Recently, Sudan III was reported to generate hazardous aromatic amines catalysed by cytochrome P450s after the induction of chemical, electrochemical and biological oxidative reactions. Some of the aromatic amines generated included aniline, 2,5-dimethylanline, ortho-anisidine, 4-aminobiphenyl, 2-methoxy-5-methlyaniline, etc. (Zanoni et al., 2013). Zanoni et al. (2013), further reported that Sudan III was mutagenic following Salmonella typhimurium TA 1535 mutagenic assay. Sudan IV (C.I. Solvent Red 24) became mutagenic after chemical reduction and microsomal activation, producing 2,5-diaminotuluene and ortho-toluidine. Para Red on the other hand was degraded predominately to 4-nitroanilin. 4-nitroaniline was reported to be highly toxic when inhaled, ingested or absorbed through the skin (Xu et al., 2010). Johnson et al. (2010) demonstrated the genotoxicity of Para Red in AHH-1 cells with genotoxicity increasing with oxidative metabolism. According to Fonovich (2013), degradation of both Sudan III and IV, following anaerobic incubation with fresh human faecal suspension lasted for more than 30 hours possibly due to their reduced solubility and availability. Further, Sudan IV induced CYP 1A1 protein and mRNA in Wister rats, although slower induction than Sudan I and III (Refat et al., 2008).

1.4.4 Sunset Yellow FCF

Sunset Yellow FCF (SY) is a sulphonated derivative of Sudan I, making it hydrophilic. SY was reported to be attributable to hepatocellular damage and renal failure (Mekkawy et al., 1998). It also causes reproductive toxicity in mice (Tanaka, 1996) and has immunotoxicity potential (Hashem et al., 2010). No mutagenic or carcinogenic

property has been reported for SY via *in vivo* and *in vitro* studies (EFSA Scientific Opinion 2009; Yadav et al., 2013). Additionally, no genotoxic effect was reported for Sunset Yellow FCF following *in vivo* micronucleus test in mice. However, the dye demonstrated some cytotoxicity as was revealed in apoptotic and mitotic cells (Poul et al., 2009). More recently, Bhattacharjee (2014) implicated Sunset Yellow FCF to induce mitotic depression in the root tips of *Allium sativum*. The report further revealed a general decline in the mitotic index with increased concentrations of Sunset Yellow FCF and incubation time (Bhattacharjee, 2014).

1.5 Analytical Methods for the Determination of Sudan dyes in food matrices

Different techniques have been used for the analysis of these azo dyes in foodstuffs over the years with majority of the methods being chromatography-based with different detector systems. The most notable is liquid chromatography coupled with different detection systems (Rebane et al., 2010).A detailed review of the methods for the determination of Sudan dyes in food is available in literature (Rebane et al., 2010; Fonovich 2013). Although these analytical techniques show high sensitivity, they suffer drawbacks such as extensive and time-consuming sample preparations, and clean-ups as well as expensive instrumentation. Recently, immunoassay-based methods have also been developed for detection of Sudan dyes (Anfossi et al., 2009; Wang et al., 2009; Xing et al., 2012) and SY (Xing et al., 2012) in foodstuffs; but these methods are very expensive although they do not require extensive clean-ups. More recently, Yu et al. (2013) developed a sensitive method employing platinum nanoparticle-modified glassy carbon electrode coupled with voltammetric detection for the analysis of Sudan I in some food samples. Although the method was sensitive, it involved steps of sample preparations and solutions using buffers, coating and modification of electrodes (Yu et al., 2013), etc., undermining the simplicity of the technique.

1.5.1 Spectroscopic Methods

The use of spectroscopic techniques for the detection of food adulteration has gained attention in recent years due to the advantages that some of these spectroscopic techniques offer. These advantages include rapid analysis, non-destructive, easy-to use, and accurate measurements. Combinations of spectroscopic techniques with multivariate methods have proven to be powerful tools for the detection of food

adulteration (Ghosh et al., 2007). Surface Enhanced Raman Spectroscopy (SERS) combined with multivariate analysis was used to screen for Sudan I in culinary spices (Di Anibal et al., 2012). UV-Visible spectroscopy coupled with multivariate classification were used as screening tools to identify the adulteration of culinary spices with Sudan I-IV dyes as well as Sudan I and blends of Sudan I + IV dyes (Di Anibal et al., 2009, 2014). Di Anibal et al. (2011) used Proton Nuclear Magnetic Resonance (^{1}HNMR) with partial least squares-discriminant analysis (PLS-DA) to detect Sudan I-IV dyes in culinary spices. Fourier Transformed Infra-red (FTIR) (Zhang et al., 2012) and Near Infra-red (NIR) (López et al., 2014; Vitale et al., 2013) have all been used in combination with multivariate techniques to detect the adulteration of food.

However these spectroscopic techniques also have some drawbacks. For instance, UV-Visible spectroscopy requires extraction of the dyes from the matrices using appropriate solvents and then filtration for sample clean-ups (Di Anibal et al., 2009, 2014). H^{1}NMR also requires the preparation of both dyes and food samples with high purity deuterated solvents before analysis (Di Anibal et al., 2011). These additional steps can make the methods lengthy and costly. Further, the above-mentioned spectroscopic methods are unable to give information about the levels of adulteration or contamination of these foodstuffs with the azo dyes. Such additional analytical steps are avoidable in the use of a spectrometric method such as X-ray fluorescence spectroscopy (XRF) which measures materials in solid, powder and liquid states with very simple and fast sample preparation.

1.6 X-rays and X-ray fluorescence (XRF)

X-rays can be classified as electromagnetic waves with associated wavelengths, or photons with energies. X-rays have wavelengths and energies between γ-rays and ultraviolet light. The wavelengths range from 0.01 to 10nm, corresponding to energies ranging from 0.125 to 125keV (Brouwer, 2010).

XRF spectroscopy is a fast and non-destructive multi-elemental physical analytical technique which can measure the chemical element compositions of materials based on their characteristic radiations. XRF has the capability of measuring all elements of the

periodic table from beryllium to uranium qualitatively, semi-quantitatively and quantitatively of solids, powders and liquids with very high accuracy and reproducibility. XRF measures concentrations in the sub-parts-per-million (ppm) up to 100%, with typical limits of detection from 0.1 to 10ppm. The materials subjected to XRF analysis can be solids such as glass, ceramics, metals, rocks, plastics, or liquids, like petrol, oils, paints, blood or even wine (Bertin, 1978; Jenkins, 1974).

1.6.1 XRF Principle

The XRF principle is based on Bohr's Atomic Model. As shown in Figure 2, when a material is irradiated with high energy X-rays, one or more electrons in the orbitals of the atoms of the chemical elements of that material or sample can be dislodged, creating a vacancy in the inner orbitals of the atom which becomes unstable. This phenomenon is called the "photoelectric effect" and the ejected or dislodged electron called "photoelectron". The atom regains its stability by filling its lower energy orbital(s) with electron(s) from a higher energy orbital, in the atom, releasing energy equal to the energy difference between the two orbitals involved (Bertin, 1974; Jenkins, 1978).

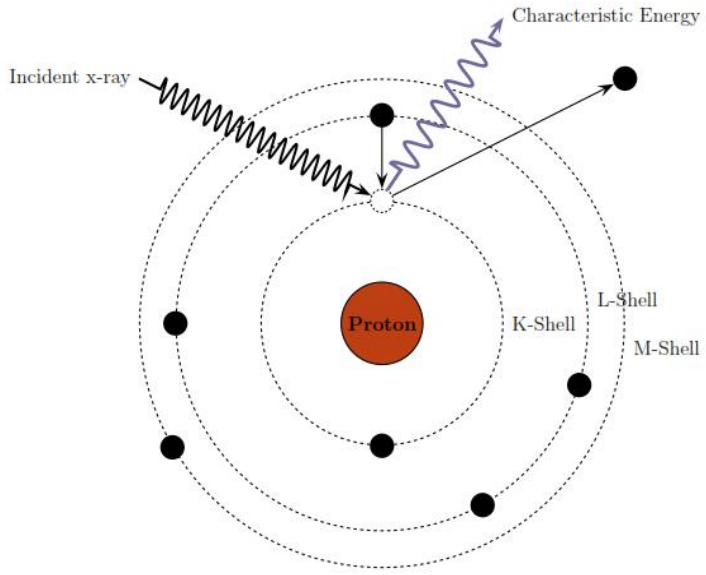

Figure 2: XRF generation diagram

The energy released can either be emitted in the form of X-ray or transferred to another atomic orbital or shell electron (Auger effect). The energy that may be released as X-

ray is called X-ray fluorescence, whose yield is dependent on the atomic number (Z) of the element and the orbital or shell in which the 'vacancy' or 'hole' occurred. The energy or wavelength of the X-ray generated is very characteristic for the element from which it is emitted, and such radiation is called *characteristic X-rays.*

1.6.2 Interactions of X-rays with samples

In addition to the photoelectric effect which produces the emission of characteristic radiation of elements present in the sample, X-ray scattering also occurs when incident X-rays collide with sample elements either as Compton or Rayleigh scattering effects (Figure 2). Other interactions which may also occur following X-ray bombardment include X-ray absorption and secondary enhancement. The fluorescence (characteristic radiation) due to photoelectric effect, Compton and Rayleigh scatters depend on the thickness (d), density (ρ) and composition of the material and on the energy of the incident X-rays (Brouwer, 2010).

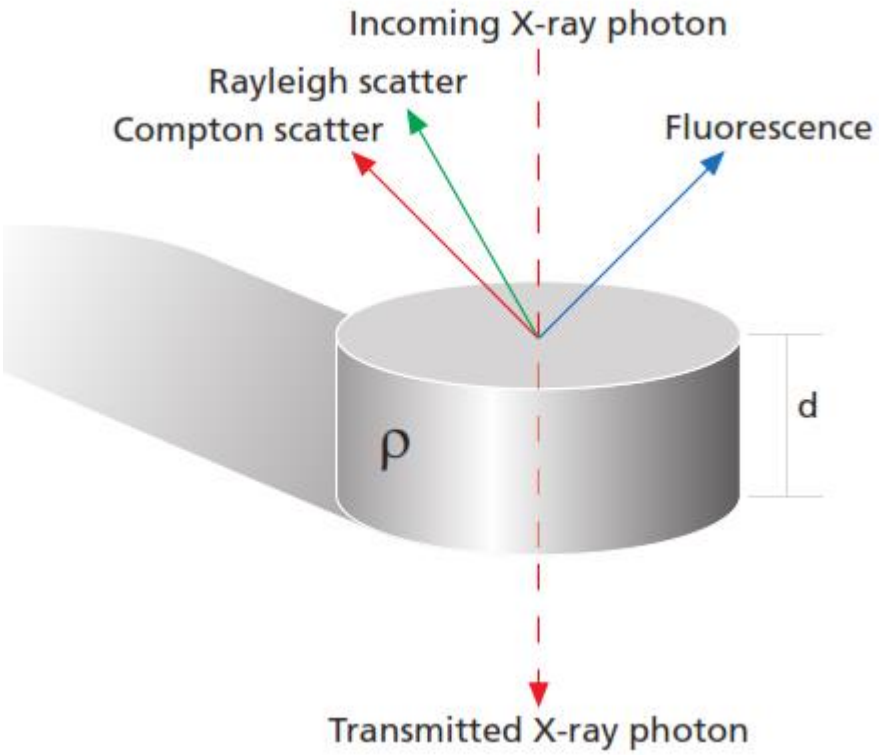

Figure 3: X-ray interactions at sample level (Adopted from Brouwer, 2010).

1.6.2.1 Photoelectric effect, Compton (inelastic) and Rayleigh (elastic) Scattering

The interaction that is observed when energetic photons such as high energy X-rays interact with matter is dependent on the energy of the incoming photon, the atomic number (Z) of the elements and the binding energy of the electrons in the elements.

Photoelectric effect, which produces the X-ray fluorescence, occurs when the energy of the incoming photon (incident radiation) is just above the binding energy of the electrons in the shells or orbitals of the elements present in a sample.

Compton scattering occurs when energy of the incident radiation is much higher than the binding energy of the electrons in the elements. This type of collision with incident X-rays produces incoherent scattering (Brouwer, 2010). During this collision, incident X-ray particles (photons) transfer their energy to the electrons leading to loss of energy (inelastic collision) and momentum. Samples mainly composed of low atomic weight (light matrix) are prone to Compton scattering effects resulting higher intensities of the Compton scatter peak with low Rayleigh scatter peak intensity. Conversely, if the energy of the incident radiation is less than or equal to the binding energy, Rayleigh (elastic) scattering occurs. When incident X-rays collide with tightly bound electrons in the inner shells of elements present in a sample material, the electrons remain in their atomic orbitals but oscillate at the same frequency as the incident X-ray and releases radiation at the same energy as the incident X-ray. There is no energy loss. However, momentum is lost as the direction of the incident X-ray is changed. Heavy atomic weight elements give rise to Rayleigh scattering.

1.6.3 Nomenclature of X-ray lines in XRF

The energy of an emitted characteristic X-ray corresponds to the difference in the energy levels or orbitals involved. The atomic orbitals or shells are labelled with letters K, L, M, N, etc. with the innermost shell being the K-shell. A K-radiation is defined as the radiation released when replenishing the K-shell, and L-radiation to that released when replenishing the L-shell (Figure 4).

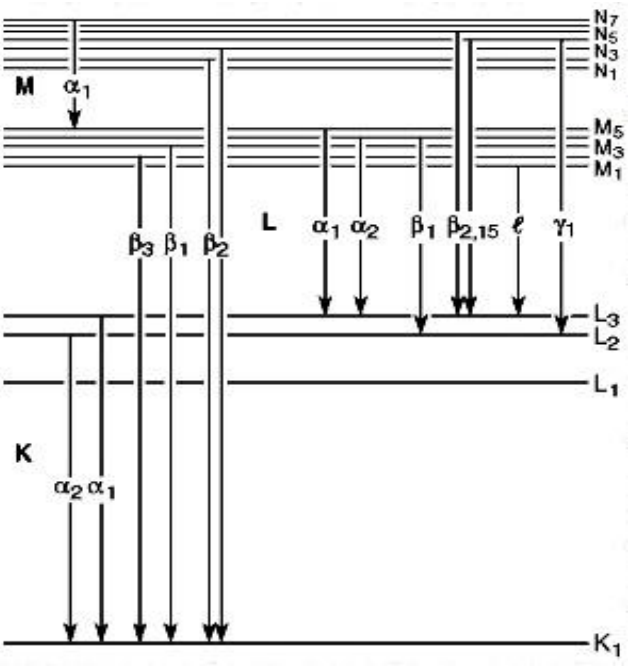

Figure 4: Characteristic X-ray lines labelling
(http://www4.nau.edu/meteorite/Meteorite/Images/Siegbahn.jpg)

For the full labelling of an emitted X-ray line, additional information stating which shell the electron filling the vacancy or 'hole' comes from is needed. The Greek letters, α, β, χ, etc. are used for that with the numbering 1, 2, 3, etc. differentiating between the various shells and sub-levels (Brouwer, 2010).

There are only a limited number of ways in which higher orbital electrons fill the vacancies of dislodged lower energy electrons. Figure 3 shows some major transitions which give rise to different types of characteristic radiations. The horizontal lines represent the energy levels in the atom whiles the vertical line represent the possible transitions. The main transitions are given names: Kα1 is transition from L3 to K, Kα2 an L2 to K transition, Kβ1 an M to K transition, Lα1 an M to L-shell transition, etc. The wavelength of a characteristic X-ray fluorescence of an atom due to a particular transition can be calculated from Planck's Law:

$$\lambda = \frac{hc}{E} \qquad (1)$$

where λ and E are the wavelength and energy of the fluorescent radiation, and h and c are Planck's constant and the speed of light respectively.

1.6.4 Wavelength-Dispersive X-ray Fluorescence (WDXRF) Spectroscopy

Wavelength dispersive X-ray fluorescence (WDXRF) is a configuration of XRF spectroscopy which analyses the wavelength of the characteristic X-ray to determine the elemental composition of material or samples has been widely employed in the food and pharmaceutical industries for multi-elemental analysis. WDXRF offers additional advantages over other spectroscopic techniques that have been used for the determination of Sudan dyes in food. They include multi-elemental analysis, direct measurements on the sample (solid or liquid samples, loose powders or pressed into pellets) without any chemical treatment, avoiding lengthy and laborious process of preparation, particularly in cases of high sample throughput, and sample contamination. The short analysis period and the ease of use of this technique, combined with low detection limits, are others advantages of WDXRF spectrometry (Yellepeddi & Thomas, 2006).

WDXRF has been applied in the food and pharmaceutical industries for numerous purposes. They include the classification of vanilla samples (Hondrogiannis et al., 2013) and cumin (Hondrogiannis et al., 2012) samples according to their geographical origins based on their elemental compositions with discriminant analyses. Perring et al. (2005) determined the levels of macroelements Na, K, Mg, P, Cl, and Ca; trace elements Zn, Mn and Fe in infant cereals using WDXRF. Additionally, Gonçalves et al. (2011) used WDXRF to analyse Cu, Zn, Fe and Cr impurities in final drug products demonstrating the appreciable linearity, precision and accuracy of the analytical method in a given concentration ranges.

So far, the ability of WDXRF spectroscopy to detect and predict the levels of adulteration of culinary spices with Sudan dyes is yet to be reported in literature. Given the ability of the WDXRF spectroscopy to measure both organic and inorganic matrices coupled with better spectral resolution and ease of use, this present study aimed to evaluate the use of WDXRF as a screening tool to detect and predict the levels of adulteration of culinary spices with Sudan I, III, IV, Para Red and Sunset Yellow FCF.

1.9 Aim and Objectives

Due to the carcinogenicity of Sudan dyes, they have been banned from use as food colorants in many countries and regions including the EU (EFSA Scientific Opinion, 2005). The EU Rapid Alert System for Food and Feed (RASFF) reports of the presence of Sudan dyes in various foods in member countries, since Sudan I was detected in the EU in May 2003 (RASFF, 2005). EU member countries have been entreated to establish uniform controls at the points into the Community to monitor entrance of imported food into (Commission Decision 2009). In such instances, screening methods would be appropriate for the control and monitoring of goods or products instead of analytical reports for consignments of imported products into the Community.

To this end, the present study aims to develop a feasible, rapid and simple method for detecting the levels of adulteration of culinary spices with illegal dyes such as Sudan dyes, using the WDXRF technique.

The specific objectives included:

i. Differentiation between the different spice samples adulterated with the different illegal dyes based on the WDXRF spectral features (Compton and Rayleigh scatters) of the adulterated samples using logistic regression and discriminant analysis.
ii. Development of models based on the Compton and Rayleigh ratios and well as intensities of the Rh Compton and Rh Rayleigh scatters for the prediction of spice's adulteration levels.
iii. Determination of the best predictors and/or the best model to predict the levels of adulteration of spices.

2. MATERIAL AND METHODS

2.0 Reagents and Samples

Sudan I (*catalogue no: 103624, Lot STBC3001V*); Sudan III (*catalogue no: S4131, Lot MKBQ6917V*); Sudan IVa (*catalogue no: 198102, Lot MKBJ2291V*); Para Red *(catalogue no: 100994, Lot MKBQ2670V*) and Sunset Yellow FCF (*catalogue no: 465224, Lot MKBJ9434V*) all of technical grade were purchased from SIGMA-ALDRICH CHEME (Lisbon, Portugal). Sudan IVb (*catalogue no: A12181, Lot 10164322*) was purchased from Alfa Aesar® Lisbon, Portugal.

Branded paprika and sweet pepper were purchased from local market in Almada, Portugal.

2.1 Sample Preparation

3g paprika and sweet pepper each prepared in triplicate were used as sample blanks for each measurement. 2.4-2.7g of Sudan IV, 3g each of Para Red and Sudan III, 2.1-2.5g of Sudan I, and 2.7-2.9g of Sunset Yellow FCF were weighed and analysed for the elemental composition of the dyes. In addition to the blank matrices and the 100% dyes samples, fourteen (14) different assay points at concentrations of 0.5, 1, 2.5, 5, 7.5, 12.5, 15, 20, 25, 30, 35, 40, 45, and 50 percent dyes (w/w) in triplicates, making a total of 48 samples per dye per matrix were prepared for the study. These concentration ranges were chosen to cover all possible levels of adulteration of the spices. Sudan I adulteration levels of about 4,000ppm or more were detected in chilli samples imported from Mumbai. Besides, at least, about 1000 ppm of Sudan I is needed to impact the visual appearance of chilli powder. It is also reported that concentrated Sudan oil solutions, of several percentages for example, 5% to 10% (50,000-100,000 ppm), are prepared and blended with other powdered samples to impact the Sudan colours to these spices (ASTA, 2005). Before been analyzed on the WDXRF spectrometer, all samples were homogenized in borosilicate glass mortars and then transferred into high-density polyethylene cups with 35.8 mm diameter assembled with a 4 μm Prolene film.

2.2 WDXRF Analysis

All measurements were done in a 4kW commercial WDXRF system (Bruker S4 Pioneer) with maximum voltage and current set at 60kV and 50mA, respectively. Semi-quantitative standardless measurements were done in Helium mode, using a Rh X-ray tube fitted with a 75 µm Be window and a 34 mm diameter collimator mask. Cellulose ($C_6H_{12}O_6$) powder was chosen to simulate the matrix. Spectral data was acquired using SpectraPlus Software Version 1.7.

Semi-quantitative standardless mode was chosen for the WDXRF analysis because the components of the contaminated or adulterated samples are not known hence. The semi-quantitative mode produces useful spectral features like the Compton and Rayleigh scatter intensities as well as their derivative ratios, which will not be significantly different if quantitative mode was used. Besides, quantitative modes would require calibration of the system for the elements present in the samples. Since the elemental compositions of the adulterated (or contaminated) spices samples were unknown, system calibration could not be performed and quantitative mode not useful.

2.3 Statistical Analysis

Data analyses were done using STATGRAPHICS Centurion XVI Version 16.1.11 from StatPoint Technologies Inc. The Compton and Rayleigh scatters as well as their derivative ratios were used for all statistical works.

Similarly, as already explained for the choice of the semi-quantitative standardless mode for WDXRF analysis, the Compton and Rayleigh scatter intensities as well as the Compton and Rayleigh ratios are quantities that are always present in WDXRF spectra hence were used for the statistical analysis. Additionally, the concentrations of the elements in the spice samples could not be used since no specific calibration was prepared for the elements. Further, depending on the geographical location from which the spices were cultivated and adulterated (taking into account the purity of the dyes), it is evident that both spice samples and dyes would have different elemental compositions which would be a limitation in the method.

2.3.1 Multivariate Classification Techniques

Multivariate classification techniques were employed to predict the types of spice adulteration prior to prediction of the levels of adulteration using multiple regression analysis. Two different multivariate classification techniques: logistic regression analysis and discriminant analysis were used to develop models to predict the type of adulterant in reported cases of adulteration of paprika and sweet pepper. These were the initial steps of the study after which models would be developed using multiple regression analysis, to predict the levels of adulteration of the spices with Sudan dyes, Para Red, and Sunset Yellow dyes. Logistic regression and discriminant analysis classification techniques were chosen to complement each other, having in mind the limitations of the techniques: binary logistic regression classifies samples only into two groups (it cannot classify samples into more than two groups, unless in multiple logistic regression) whereas discriminant analysis can classify samples into more than two groups or classes.

2.3.1.1 Logistic Regression Analysis

A total of 210 samples comprising of triplicates of adulterated paprika samples with Sudan I, III, IV, Para Red, and Sunset Yellow FCF dyes with adulteration levels between 0.5% and 50%, were used for the logistic regression. 126 samples belonging to paprika adulterated with either Sudan I, III, and IV were classified as ‘Cases’ (Sud) with a binary code of ‘1’ whereas the remaining 82 samples adulterated with Para Red and Sunset Yellow FCF (Non-sud) were classified as ‘Non-cases’ with a binary code of ‘0’ for the logistic regression. All four variables; Compton and Rayleigh intensities, Compton and Rayleigh ratios were used to develop the model for future predictions.

2.3.1.2 Discriminant Analysis

Firstly, the 210 samples were divided into two main groups, as was done for the logistic regression. Group ‘Sud’ comprised of 126 samples made up of Sudan I-, III-, and IV-adulterated paprika whereas the remaining 84 Para Red and Sunset Yellow adulterated paprika samples were categorized as group ‘non-Sud’. This classification model was compared with the binary logistic regression model.

Secondly, a third group was introduced by splitting the ‘non-Sud’ group into two sub-groups making a total of 3 groups or classes. The new groups or classes were as

follows: class ‘Sud’ for Sudan I, III and IV-adulterated paprika samples, class ‘PRed’ for Para Red-adulterated paprika, and class ‘SY’ corresponding to Sunset Yellow-adulterated paprika samples. Similarly, all four variables which were the Compton and Rayleigh scatter intensities as well as their derivative ratios were used to develop the models.

2.3.2 Multiple Regression Analysis

Three multiple regression models: *Model **A*** based on the Compton and Ryleigh ratios; *Model **B*** based on the Rh Compton and Rayleigh scatter intensities; and *Model **C*** or the full model based both the ratios and the scatter intensities were prepared for each class of spice adulteration (7 classes in all). Multiple regressions with stepwise backward selection method using the pre-defined predictors were prepared. A total of 45 data sets per sample, including the blank spices (0% adulteration) were used to prepare the models. Influential points and points with unusual Studentized residuals (>3) were removed from the dataset for optimization of the model.

3. RESULTS AND DISCUSSION

3.0 WDXRF Spectra details of pure spices and dyes

3.0.1 Compton Ratio

The Compton ratio is an estimate based on the measured intensity of non-coherent scattering by light elements in the sample compared to the theoretical intensity based on the simulated matrix (cellulose, $C_6H_{12}O_6$). It is greatly affected by the amount of lighter atomic weight elements present in a sample and which cannot be measured by XRF. A ratio close enough to 1 is desirable. The Compton ratios for the spices and dyes (Figure 5) indicate that the matrix simulation in the study was credible. This could significantly minimize matrix-mismatched associated errors in the experiment. Paprika and sweet pepper had values closer to 1. These Compton values for paprika and sweet pepper were expected since they are largely composed of cellulose and light elements. Among the dyes, Sudan III and Sudan IV had the highest and lowest ratios of 1.26 and 0.90, respectively. The Compton ratio for Sudan III was expected given the observed 'lighter' nature of the dyes during the experiment. This could suggest that Sudan III dye composed of higher concentration of lighter elements than the other dyes and, the opposite is true for the Sudan IV dyes.

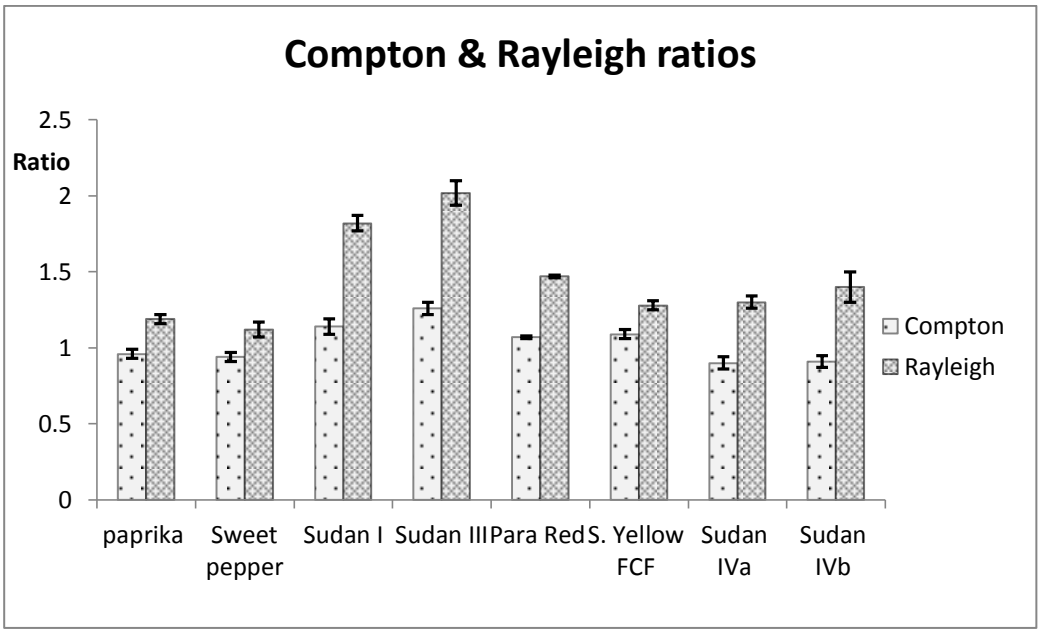

Figure 5: Compton and Rayleigh ratios of the pure spices and dyes. Paprika and sweet pepper had similar ratios. Sudan III and I dyes had the highest Compton and Rayleigh ratios. Sudan IVa and IVb dyes (from Alfa Aesar® and Sigma-Aldrich®, respectively), had the lowest Compton and Rayleigh among the dyes ratios. A ratio close to one is desirable for matrix simulation. The highest Compton ratio deviations were observed for Sudan I and III dyes whereas Para Red dye had the least deviations for both Compton and Rayleigh ratios.

3.0.2 Rayleigh Ratio

The Rayleigh ratio compares the intensity of coherent scattering as due to heavier elements in the measured sample to that of the cellulose matrix. Matrices composed of heavier atomic weight elements (heavier matrix) are more likely to produce Rayleigh scattering than lighter matrices. In relation with the Compton ratio, the Rayleigh ratio gives information regarding the appropriateness of matrix simulation considering heavier elements. As shown in Figure 2 above, it was observed that Rayleigh ratios of the unadulterated spices (paprika and sweet pepper) as well as the pure dyes, with the exception of Sudan I and III, were closer to 1, with average ratios between 1.12 and 1.47. Paprika and Sweet pepper had average ratios of 1.19 and 1.12 respectively. These observations support our deduction that the matrix simulation in this study was appropriate as already revealed by the Compton ratios. However, the Rayleigh ratios for Sudan III and I dyes were very high (2.02 and 1.82, respectively) indicating that Sudan III and I contain lesser amounts or concentrations of heavier elements than other spices This issue can be resolved by the use of a more lighter matrix than cellulose, such as the C5 sugars (hemicellulose). Sunset Yellow FCF had a low ratio of 1.28 among the dyes followed by Sudan IVa and IVb dyes. These findings were also consistent with the Compton and Rayleigh scattering intensities of the dyes (Figure 5).

3.0.3 Compton and Rayleigh Scatter Intensities

The intensity of an X-ray quantum is defined as the number of X-ray quanta per unit time recorded at the detector as pulses per second or counts per second (Cps). It contains the information about the concentration of the emitting elements present in a sample. Matrices high in lower atomic weight elements (lighter matrix) are more susceptible to Compton scattering resulting in greater intensity of the Rh Compton scatter quanta reaching the detector. Conversely, Matrices with higher atomic weight elements (heavier matrix) are prone to Rayleigh scattering resulting in a greater intensity of the Rh Rayleigh peaks recorded in the detector.

Sudan I and III had the lowest Rayleigh scatter intensities of 74.5 and 74.6KCps, respectively whereas Sunset Yellow FCF had the lowest Compton scatter intensity of 303.5KCps. In all spices and dyes, the Compton scatter intensities were higher than the Rayleigh scatter intensities, indicating that both spices and the dyes used in the study composed largely of lighter elements. Based on the Compton and Rayleigh ratios (Figure 5) as well as the scattering intensities of the dyes and spices (Figure 6),

WDXRF exhibits the potential of determining Sudan dyes adulteration in paprika and sweet pepper when the appropriate multivariate classification techniques are applied.

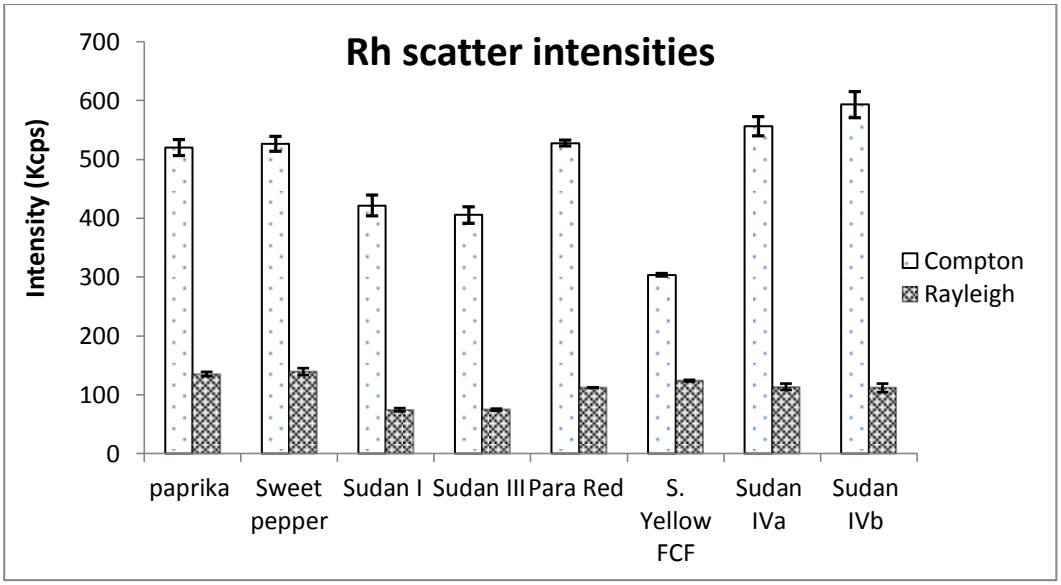

Figure 6: Compton and Rayleigh scatter intensities of pure spices and dyes.Sudan Iva and IVb are Sudan IV dyes from Alfa Aesar® and Sigma-Aldrich, respectively. The highest Compton scattering was observed for Sudan Iva and IVb dyes whereas Sunset Yellow FCF had the lowest Compton scatter intensity among the dyes. Paprika and Sweet pepper had similar Compton and Rayleigh scatter intensities, consistent with the Compton and Rayleigh ratios. Sudan I and III had the lowest Rayleigh scatter intensities, corresponding to the highest Rayleigh ratios in those dyes.

3.0.4 Percentage 'Matrix'

In WDXRF spectra, 'matrix' refers to the composition of samples or material that is not measured by the technique. The '% matrix' can be defined as the percentage of other components in the sample material apart from the measured elements. In our experiment, the 'matrix' is composed of lower atomic weight elements (Z<11) as well as other sample components that cannot be measured by the WDXRF technique together with any other sample composition due to the intrinsic limitation of the WDXRF spectrometer. By this definition, they include elements such as Ne, F, O, N, C, B, Be, He, etc. Table 1 shows the percentage 'matrix' of the dyes and spices used in this study. The results indicate that nearly 5% of the elemental compositions of paprika and sweet pepper were detected by the WDXRF spectrometer. About 2% of the elemental compositions of Sudan III, Para Red, Sudan IVa dyes were measured whilst less than 1% of the elemental compositions of Sudan I and Sudan IVb were measured by the WDXRF technique. Approximately 26% of the composition of Sunset Yellow

FCF was measured by the WDXRF technique indicating that Sunset Yellow FCF contains a higher percentage of 'measureable' elements than the other dyes.

Table 1: Percentage 'Matrix' of pure spices and dyes analysed in the study

Sample	Matrix (%)	Std. deviation (n)
Paprika	95.7	0.2 (15)
Sweet pepper	95.4	0.1 (6)
Sudan I	99.6	0 (3)
Sudan III	98.2	0.1 (3)
Para Red	98.4	0 (3)
Sunset Yellow FCF	73.9	0 (3)
Sudan IVa	98.0	0.4 (3)
Sudan IVb	99.4	0 (3)

Sudan IVa and *IVb* refer to Sudan IV dyes purchased from Alfa Aesar® and Sigma-Aldrich Chemie, respectively. *n* refers to the sample size.

3.0.5 Elemental Compositions of the pure spices and dyes

The elemental compositions of paprika, sweet pepper and the dyes obtained using the standardless semi-quantitative methods in the WDXRF analysis are shown below. The estimated concentrations as well as the statistical error (instrumental) associated with the measurement are summarized below. It must be emphasised that the concentrations of the elements (ppm) are estimated values whose exact amounts can only be obtained through quantitative analysis following the development of calibration models for the elements present in the samples. However, giving the magnitudes of the statistical errors associated with these estimations, it can be inferred that these concentrations are near accurate, for some of the elements, especially the elements with statistical errors at 5% and below. Elements in which the concentrations had estimated statistical errors up to 10% could be referred to as 'possibly present' in the sample. Statistical error above 10% associated with the estimated concentration of an element makes the presence of an element in a sample doubtful with high uncertainties.

3.0.5.1 Elemental Compositions of pure Paprika and Sweet pepper

Paprika and sweet pepper had very similar elemental compositions. Ten (10) elements were detected in both paprika and sweet pepper with Br exclusively in sweet pepper. The elemental compositions of paprika and sweet pepper are summarized in Table 2. The most predominant element in both spices was K at concentrations of 26,154.2±924.4 ppm and 29,206.7±326.6 ppm for paprika and sweet pepper, respectively. The concentrations of Cl, P, Mg, S, Ca, and Si, were also predominant in both spices. However, concentrations of Ca were significantly different between paprika (2,648.3±96.8 ppm) and sweet pepper (1,713.3±25.2 ppm). Al, Fe, and Cu were present at trace levels in both spices. In addition, trace amounts of Br was also detected in sweet pepper. Although, these elemental concentrations were obtained in semi-quantitative mode, without specific calibrations for the elements (as already stated), these concentrations are accurate, given the lower statistical errors associated with the estimations. The amounts of elements detected in paprika and sweet pepper were consistent with the Compton and Rayleigh ratios, as well as Compton and Rayleigh scatter intensities obtained for both spices. These values were also expected since paprika and sweet pepper belong to the same family of plants.

Table 2: Elemental compositions of pure paprika and sweet pepper

Element	**Concentration (x10^4 ppm)**		**Stat. error (%)**	
	Paprika	***Sweet p.***	***Paprika***	***Sweet p.***
K	2.616±0.092	2.921±0.033	0.2	0.2
P	0.357±0.019	0.356±0.004	1.2	1.7
Cl	0.340±0.016	0.362±0.004	1.3	1.3
Mg	0.287±0.018	0.277±0.002	1.6	1.7
Ca	0.265±0.010	0.171±0.003	0.8	1.0
S	0.223±0.014	0.218±0.002	1.1	1.1
Si	0.115±0.008	0.117±0.002	2.8	2.7
Al	0.033±0.002	0.035±0.002	6.9	6.6
Fe	0.027±0.001	0.025±0.0003	1.2	1.2
Cu	0.003±0.0002	0.003±0.0001	4.9	4.9
Br	**	0.005±0.0001	**	2.8

Sweet p refers to sweet pepper and *Stat. error*, the statistical error associated with the estimation of the concentrations of the elements present in the samples by the WDXRF instrument.

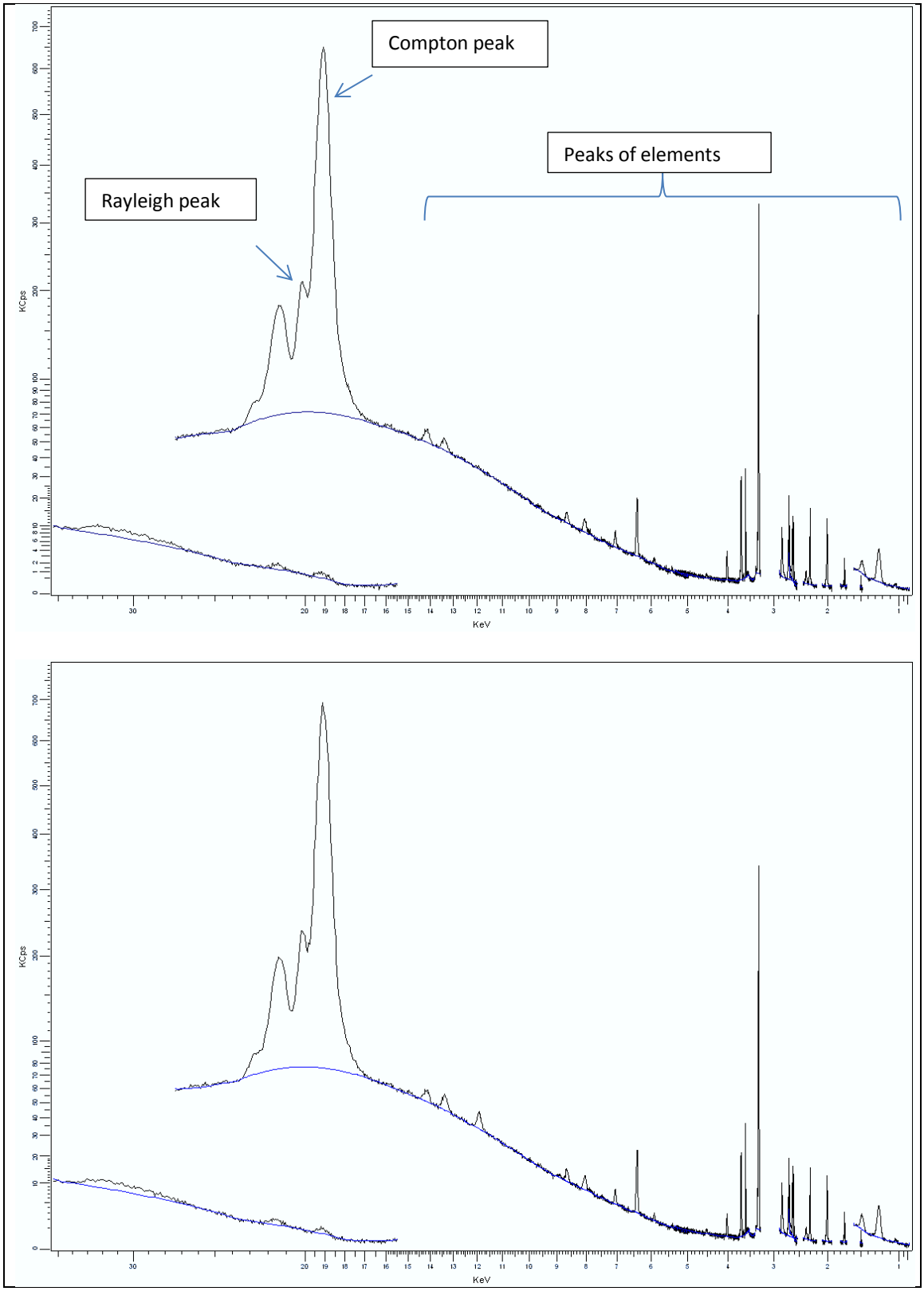

Figure 7: WDXRF spectra of pure (unadulterated) paprika (top) and sweet pepper (bottom).

3.0.5.2 Elemental composition of Sudan I and Sudan III dyes

The elemental compositions of pure Sudan I and Sudan III dyes are presented in Table 3. Nine (9) elements were detected in Sudan I whereas eight (8) were detected in Sudan III. The most predominant element Sudan I dye was Cl at an estimated concentration of 1,013.3±30.6 ppm, followed by Ca (871.3±20.0 ppm) and Na (840.0±26.5 ppm). Na (6,946.8±270.1 ppm), Cl (6,426.7±30.6 ppm) and Ca (2,660.3±34.6 ppm) were the most predominant elements in Sudan III dye. S, Mg, Si, Fe, and K were detected at trace levels in both dyes. In addition, Al was detected in Sudan I at a trace level of 260.0 ppm but was not detected in Sudan III. These findings were also consistent with the Compton and Rayleigh ratios, as well as the scatter intensities obtained for Sudan I and III dyes. The very light nature of the Sudan III powder observed during the study is explained by the fact that it largely composed of light elements Na (Z=11), Cl (17) and Ca (20).

Table 3: Elemental compositions of Sudan I and III dyes.

	Concentration (x10^4 ppm)		**Stat. error (%)**	
Element	***Sudan I***	***Sudan III***	***Sudan I***	***Sudan III***
Cl	0.101±0.003	0.643±0.003	2.5	0.9
Ca	0.087±0.002	0.266±0.004	1.2	0.7
Na	0.084±0.003	0.695±0.027	10.1	2.6
S	0.028±0.001	0.030±0.001	3.3	3.3
Al	0.026±0.0001	**	7.5	**
Mg	0.021±0.001	0.052±0.002	8.8	4.6
Si	0.020±0.001	0.033±0.001	7.4	5.6
Fe	0.012±0.0001	0.032±0.001	1.7	0.9
K	0.005±0.001	0.003±0.0001	10.6	10.8

Stat. error is the statistical error associated with the estimation of the concentrations of the elements present in the samples by the WDXRF instrument.

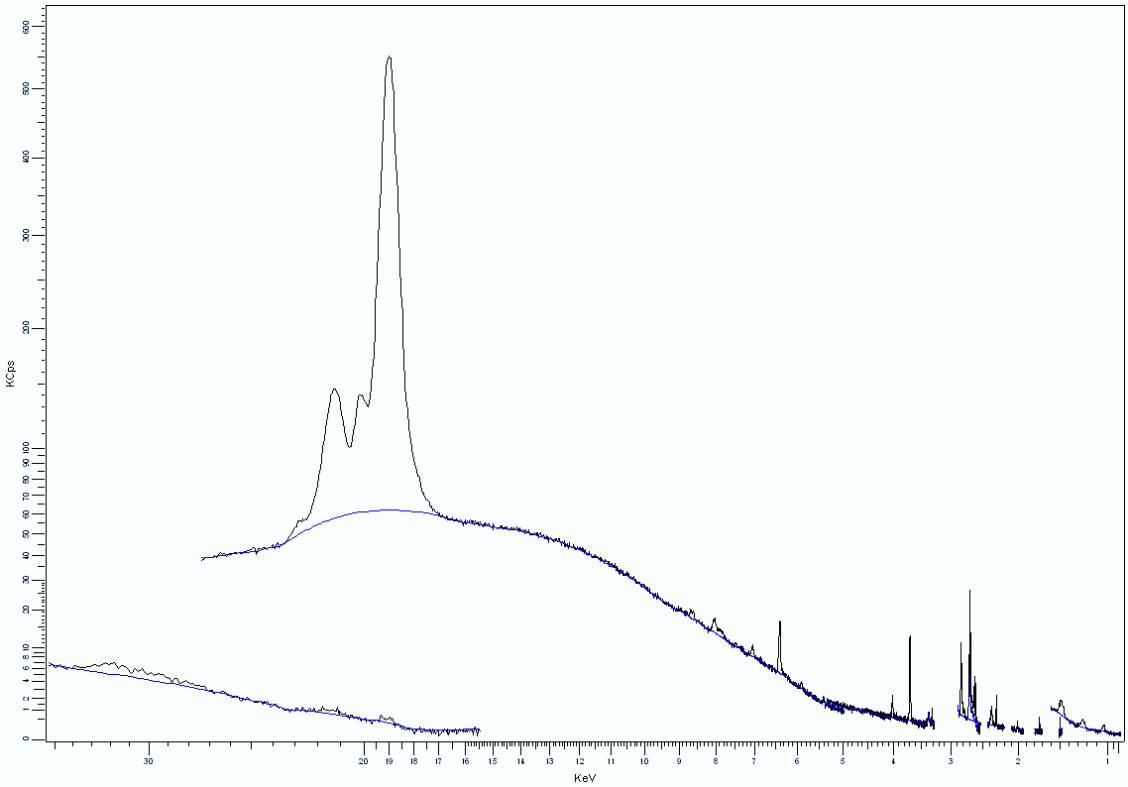

Figure 8: WDXRF spectrum of Sudan I dye.

3.0.5.3 Elemental Compositions of pure Sudan IVa and IVb dyes

Eleven (11) elements were detected in Sudan IVa dye (from Alfa Aesar®). The predominant elements were Na (8,223.3±274.3 ppm), Cl (7,340.0±205.3 ppm) and Si (1,430.0±69.3 ppm). Conversely, eight (8) elements were detected in Sudan IVb (from Sigma Aldrich) predominantly Na (1,843.3±169.2 ppm) and Cl (1,763.3±85.1 ppm). In addition to Na, Cl, Si, Fe, Ca, S, and K, which were common to both Sudan IVa and IVb dyes, Mg at 396.7±5.8 ppm, Cu at 91.0±9.5 ppm, and Ti (<50ppm) were also detected in Sudan IVa. However, the concentrations of Na, Cl, Si, Fe, and K detected in Sudan IVb were significantly lower than detected in Sudan IVa. Additionally, Sudan IVb contained Ba at a level of 887.0±15.4 ppm which was not detected in Sudan IVa. Conversely, the concentration of S detected in Sudan IVb was about twice higher than detected in Sudan IVa. These differences were expected since the Sudan IV dyes were from different manufacturing sources and they may account for the minimal differences observed in the Compton and Rayleigh ratios as well as the scatter intensities of the Sudan IV dyes.

Table 4: Elemental compositions of Sudan IV dyes.

Element	Conc. ($x10^4$ ppm)		Stat. error (%)	
	Sud IVa	*Sud IVb*	*Sud IVa*	*Sud IVb*
Na	0.822±0.027	0.184±0.017	2.4	6.0
Cl	0.734±0.021	0.176±0.009	0.9	1.8
Ba	**	0.089±0.002	**	2.0
Si	0.143±0.007	0.009±0.001	2.4	14.0
Fe	0.086±0.011	0.020±0.0001	0.5	1.2
Ca	0.081±0.005	0.053±0.001	1.3	1.5
Al	0.062±0.004	**	4.7	**
Mg	0.040±0.001	**	6.0	**
S	0.038±0.001	0.062±0.001	2.8	2.1
K	0.023±0.001	0.002±0.0001	2.7	13.8
Cu	0.009±0.001	**	1.7	**
Ti	0.004±0.001	**	9.1	**

Sud IVa and *IVb* are Sudan IV dyes purchased from Alfa Aesar® and Sigma Aldrich, respectively. *Stat. error* is the statistical error associated with the estimation of the concentrations of the elements present in the samples by the WDXRF instrument.

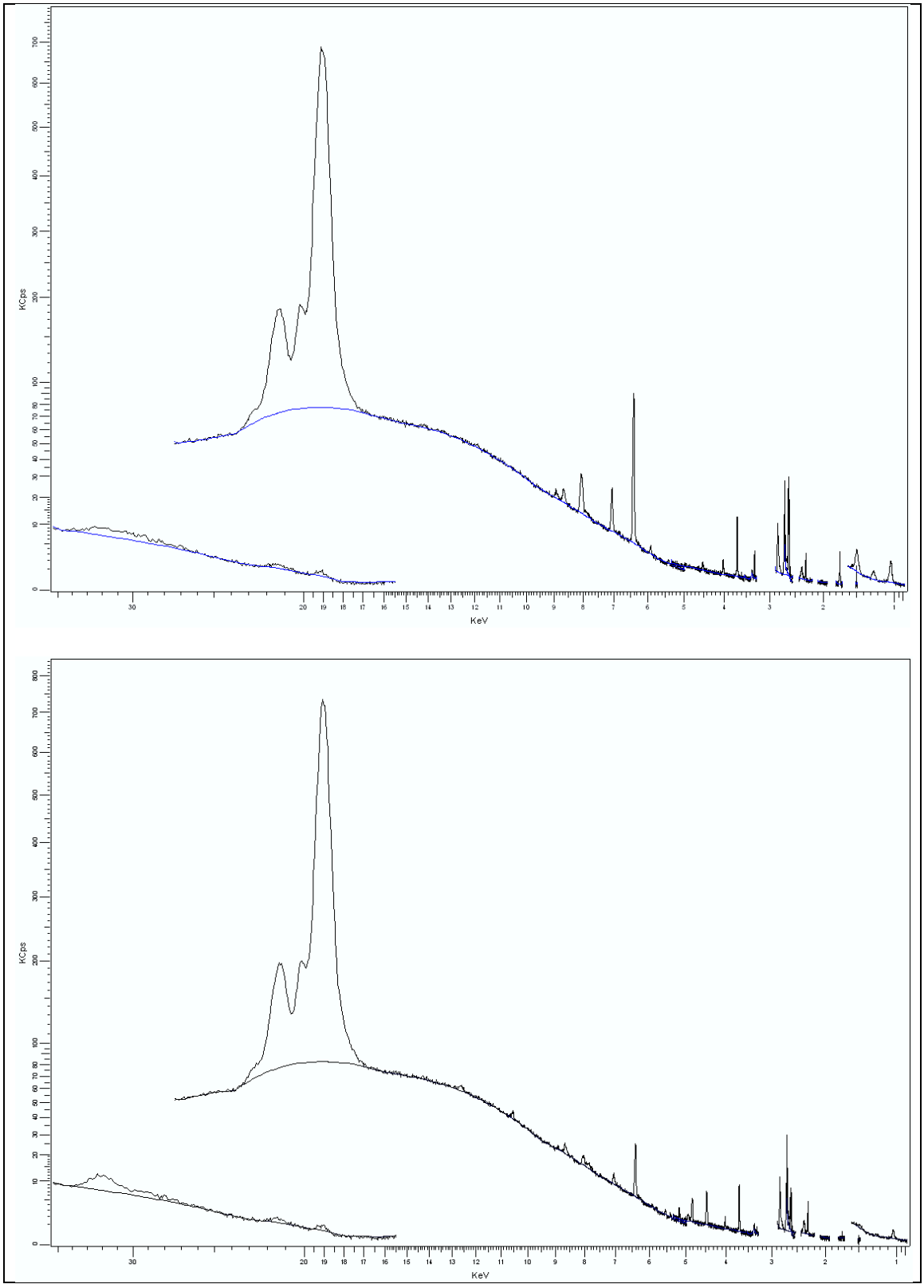

Figure 9: WDXRF spectra of Sudan IVa (top) and Sudan IVb (bottom) dyes.

3.0.5.4 Elemental Compositions of Para Red and Sunset Yellow FCF dyes

Para Red and Sunset Yellow FCF dyes are both structurally related to Sudan I. Sunset Yellow is the sulphonated analogue of Sudan I, making it highly hydrophilic. Para Red contained eight (8) elements, predominately, Cl at 7,936.7±75.1 ppm and Na at 7,256.7±80.0 ppm levels. Other elements detected in Para Red included S, Fe, Si, Ca, Br, and Cu some of which were also detected in Sunset Yellow. Seven (7) elements were detected in Sunset Yellow FCF dye. The predominant elements were S (109,200.0±1,228.8 ppm), Na (97, 866.7±2,013.3 ppm), K (43, 930.0±477.9 ppm) and Cl (9,143.3±198.6 ppm). Mg at the concentration of 729.3±7.8 and K were detected in Para Red but not in Sunset Yellow. Conversely, was also detected in Sunset Yellow in addition to the elements common to both Para Red and Sunset Yellow.

Table 5: Elemental compositions of Para Red and Sunset Yellow FCF dyes.

Element	**Concentration ($x10^4$ ppm)**		**Stat. error (%)**	
	PR	***SY***	***PR***	***SY***
Cl	0.794±0.008	0.914±0.020	0.8	1.1
Na	0.726±0.007	9.787±0.201	2.6	0.6
S	0.031±0.001	10.92±0.123	3.2	0.2
K	**	4.393±0.048	**	0.3
Mg	**	0.073±0.001	**	5.4
Si	0.010±0.001	**	12.1	**
Ca	0.010±0.0001	**	4.5	**
Br	0.005±0.0001	**	2.6	**
Fe	0.021±0.001	0.003±0.0001	1.2	8.7
Cu	0.002±0.0001	0.003±0.0001	6.5	7.7

PR and *SY* refer to Para Red and Sunset Yellow FCF dyes, respectively. *Stat. error* is the statistical error associated with the estimation of the concentrations of the elements present in the samples by the WDXRF instrument.

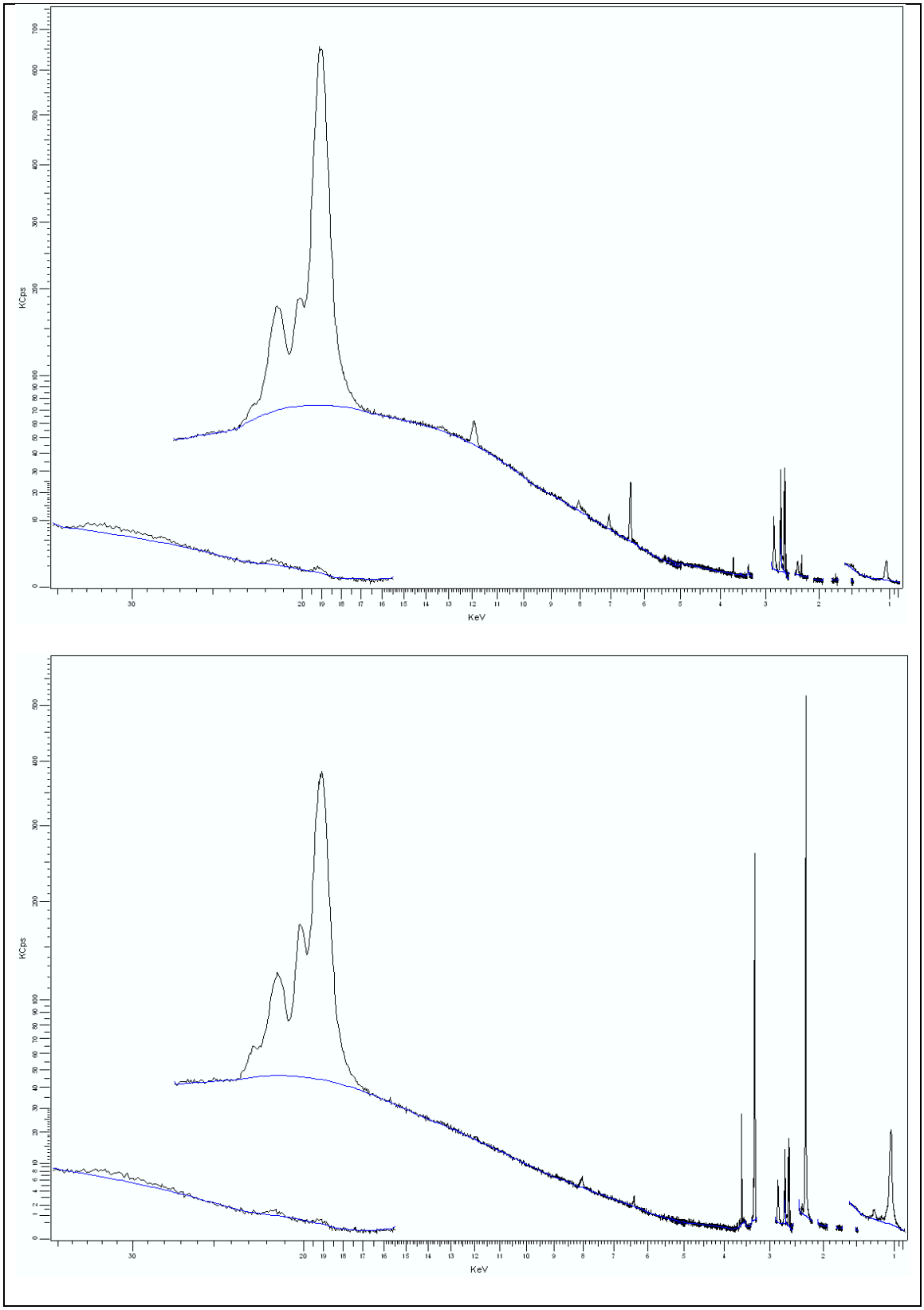

Figure 10: WDXRF spectra of Para Red (top) and Sunset Yellow FCF (bottom) dyes.

3.1 Logistic Regression (LR)

Logistic regression was employed as a classification tool to predict the type of spice adulteration prior to the prediction of the levels of adulteration using multiple regression analysis. The omnibus test for the model coefficients of the LR model revealed that the fitted model was statistically significant ($p<0.05$) at the 95% confidence interval or higher with a Chi-square (χ^2) of 145.4 and degree of freedom (df) of 4. This indicates a significant relationship between the predictors or variables (Compton & Rayleigh intensities and Compton & Rayleigh ratios) fitted in the model at the 95% confidence level. The Hosmer-Lemeshow chi-square test was non-significant ($p>0.05$) indicating that the fitting of the model was adequate. Further, the Nagelkere R^2 was good 0.675 supporting the goodness of fit of the model as revealed by the Hosmer-Lemeshow chi-square test.

The coefficients as well as the test of coefficients in the fitted logistic regression model are presented in Table 6.

Table 6: Summary of the fitted logistic regression model.

Parameter	**Estimate**	**Std. Error**	**Odds ratio**	**Likelihood Ratio Tests**		**H-L Test**	
				χ^2	*p*	χ^2	*p*
CONSTANT	282.793	60.932					
Rh Compton intensity	-0.021999	0.018479	0.978241	1.42564	0.233	7.165	0.52
Rh Rayleigh intensity	-0.950142	0.212718	0.386686	32.2257	0.000		
Compton ratio	-102.647	27.1052	≈ 0	17.576	0.000		
Rayleigh ratio	-37.0268	23.6433	≈ 0	2.48967	0.115		

H-L refers to the Hosmer-Lemeshow test of the model whereas *p* is the p-value. The odds ratio for Compton and Rayleigh ratios were approximately zero.

The likelihood ratio test (Table 6) assesses the contribution of each predictor in the fitted model. The Compton and Rayleigh ratios were the most significant contributors in the prediction ability considering the p-values of the likelihood ratios tests. However, since the ratios are derivatives of the true measured physical quantities, which are the Compton and Rayleigh scatter intensities, simplification of the model by the removal of the intensities would not be meaningful. The odds ratio is indicative of each predictor's effect on the exponential function of the fitted regression model. The odds ratio for both the Compton and Rayleigh ratios, unlike the intensities, were

approximately zero indicating negligible effects of these predictors on the exponential function of the fitted model.

Table 7: Logistic regression prediction performance, sensitivity and specificity.

Category	Size	Correct Prediction (%) *True*	*False*	*Total*	Sensitivity %	Specificity %
Case	126	112	14	83.3	88.9	75.0
Non-case	84	21	63			

Sudan I, III, and IV-adulterated paprika samples are classified as 'true' cases whereas paprika adulterated with Para Red and Sunset Yellow dyes (non-Sudan dyes or other dyes-adulterated samples) are known as 'false' cases.

In the LR classification, Sudan dyes-adulterated paprika were assigned as 'cases' (Sud) and coded '1' whereas Para Red and Sunset Yellow-adulterated paprika were assigned as 'non-cases' (Non-Sud) and coded '0'.

The prediction performance of the logistic regression model was very good with an overall correct prediction percentage of 83% (Table 7). At 0.5 cut-off value, 88.9% of Sudan dye-adulterated samples were correctly predicted whereas 75% on non-Sudan dye-adulterated samples were correctly predicted. A sensitivity of 88.9% is very good. Since Sudan dyes are the most detected in reported cases of paprika adulteration, hence 88.9% sensitivity indicates a greater prediction chance of a Sudan dye-adulterated paprika being correctly predicted. The area under the curve of the receiver operating curve (Figure 3) was 0.923 with a standard error of 0.018 indicating a prediction power of the model to be 92.3% with a 2% error rate. This is very good for the model.

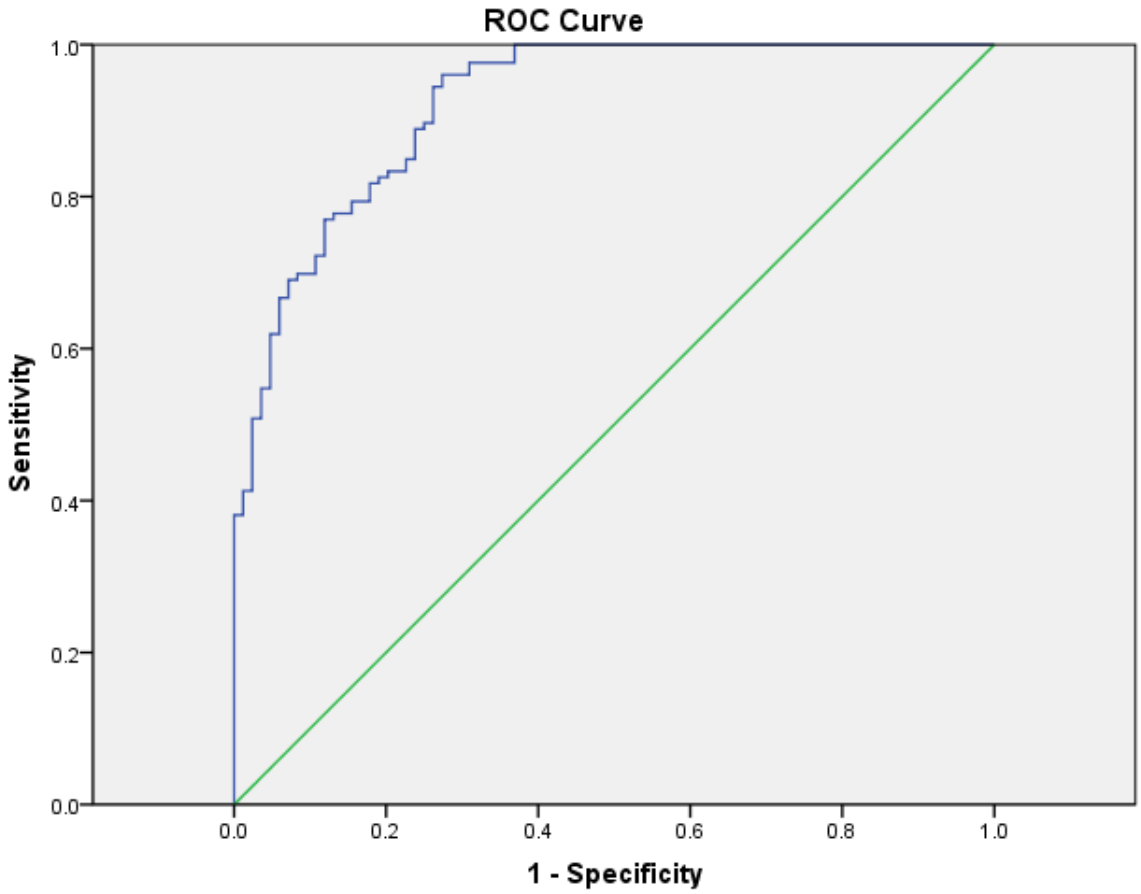

Figure 11: Receiver Operating Characteristic (ROC) curve of the logistic regression model.

The results of the logistic regression reveal the ability of WDXRF to differentiate between Sudan dye-adulterated paprika and paprika adulterated with Sudan dyes (I, III, and IV) adulterated and Para Red & Sunset Yellow-adulterated paprika with a high degree of accuracy. Further, the adequacy of the fitted model and the higher predictive power would enable future predictions of Sudan dyes-adulterated paprika samples.

3.2 Discriminant Analysis (DA)

Two different models were developed. Model A in which data were classified into two broad classes: paprika samples adulterated with Sudan I, III, and IV dyes were assigned as 'Sud' class whereas Para Red and Sunset Yellow-adulterated paprika samples were assigned 'Non-Sud' class. In Model B, a third class was introduced by dividing class 'Non-Sud' into classes 'PRed' and 'SY' for Para Red and Sunset

Yellow-adulterated paprika samples respectively. Sudan I, III, and IV-adulterated paprika samples were maintained in the 'Sud' class. Both fitted models were statistically significant ($p<0.05$) at the 95% confidence level.

Table 8: Discriminant analysis classification and discriminant functions coefficients.

Classification function coefficients					
Parameter	**Model A**		**Model B**		
	Sud	***Non-Sud***	***Sud***	***PRed***	***SY***
Compton int.	0.0166	0.0096	3.0721	3.9069	3.3374
Rayleigh int.	76.7071	77.4201	66.2494	66.3797	67.9386
Compton ratio	-269.842	-219.564	2858.18	3087.75	2604.63
Rayleigh ratio	7812.670	7843.750	5896.39	5819.74	6109.99
CONSTANT	-9688.67	-9866.95	-10442.1	-10698.8	-10493.8

Discriminant function coefficients						
Parameter	**Model A**		**Model B**			
	1_{Us}	1_S	1_{Us}	$1s$	2_{Us}	2_S
Compton int.	-0.0036	-0.1192	0.1154	2.9769	0.0427	1.1001
Rayleigh int.	0.3667	2.1687	-0.4034	-2.3838	0.2405	1.4209
Compton ratio	25.8595	1.0643	90.8421	3.6284	65.1216	2.6011
Rayleigh ratio	16.1322	0.9553	-62.3344	-3.6972	-7.4261	-0.4405
CONSTANT	-91.5015		-18.3299		-108.039	

Sud, Non-Sud, PRed, and SY refer to Sudan dyes-adulterated, non-Sudan dyes-adulterated, Para Red and Susnet Yellow-adulterated paprika samples, respectively. *Compton int.* and *Rayleigh int.* are the Compton and Rayleigh scatter intensities. *Models A* and *B* are the models discriminating two and three classes of adulterations, respectively. 1_{Us} and 1_S refer to unstandardized and standardized discriminant function 1 whereas 2_{Us} and 2_S correspond to discriminant function 2.

In model A, the single function obtained for discriminating the adulterated paprika samples into the Sudan dyes-adulterated (Sud) and non-Sudan dyes-adulterated (non-Sud) was statistically significant at the 95% confidence level with Eigenvalue of 0.916 and canonical correlation of 0.69. Similarly in model B, both discriminant functions were statistically significant at the 95% confidence level. The Eigenvalues were 2.482 and 0.761, canonical correlations of 0.84 and 0.66, with relative percentages of 76.5% and 23.5% for functions 1 and 2, respectively in model B. The Rayleigh ratio had the highest absolute classification coefficients followed by the Compton ratio in both models (Table 8) among the various adulteration classes or groups. This could be due to the variations in the Rayleigh ratios (as a function of the Rayleigh scatter intensity)

among the Sudan dyes used for adulteration as a result of varying high atomic (or middle Z) elements present in the dyes. Conversely, the Compton ratio had the highest absolute discriminant coefficients followed by the Rayleigh ratio in both models. However, the unstandardized coefficients of the discriminant functions in model B was about 4x higher than observed in model A. This could be due to the differences in the amounts light (low Z) elements present in Para Red and Sunset Yellow dyes liable to Compton scatter effect as a result of high-energy X-ray irradiation.

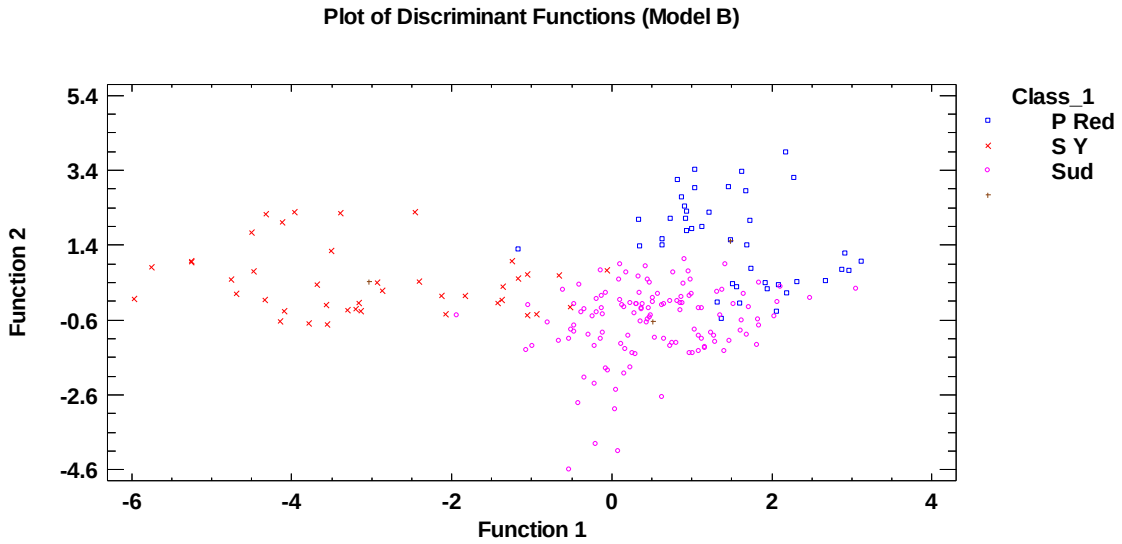

Figure 12: Discrimination of the adulterated paprika samples in DA model B. *Sud*, *P Red* and *SY* correspond to Sudan I, III, and IV-adulterated, Para Red-adulterated and Sunset Yellow-adulterated paprika samples, respectively.

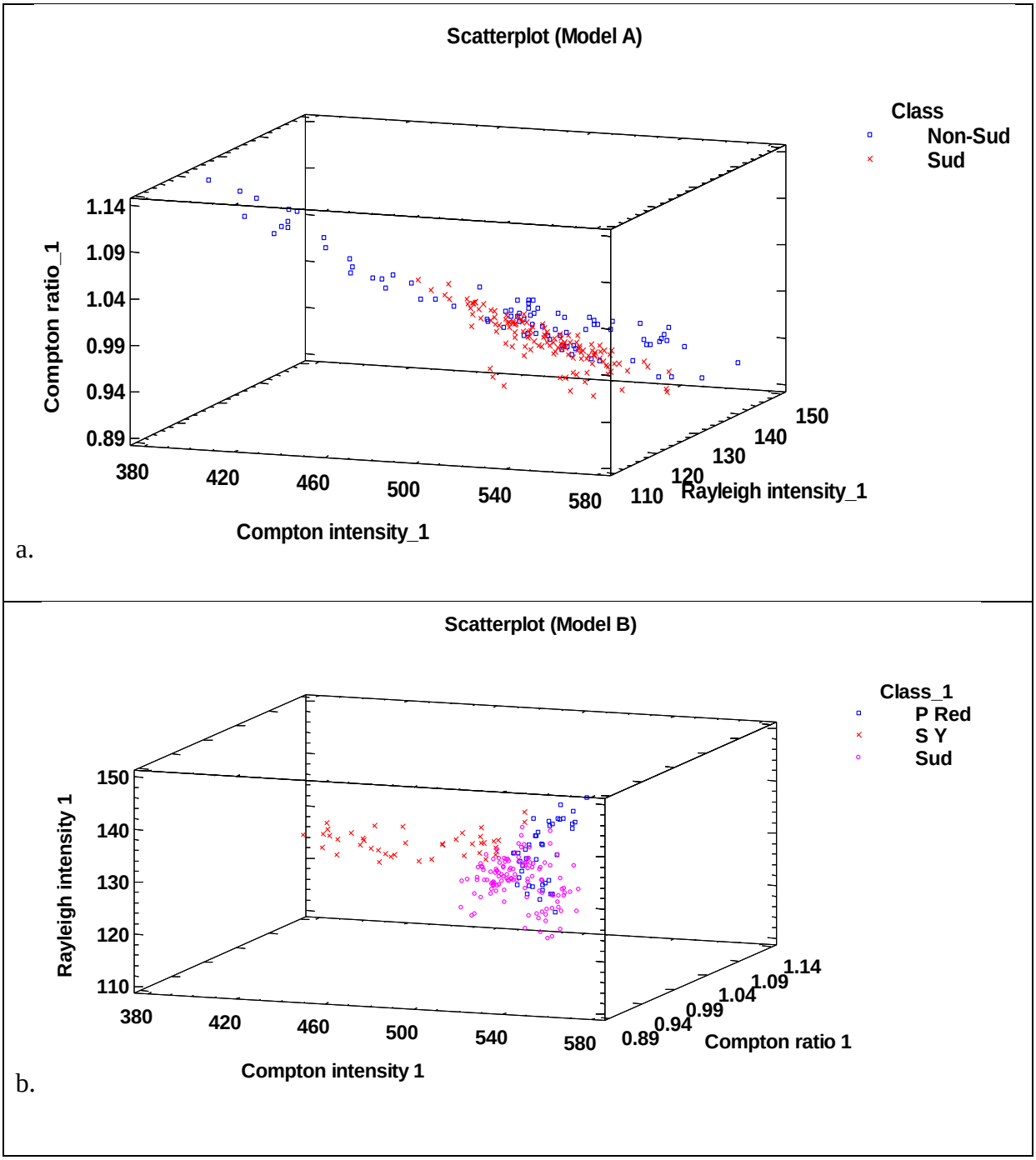

Figure 13: Scatter plot in models A (a) and model B (b). *Sud* and *Non-Sud* correspond to Sudan dyes and non-Sudan dyes-adulterated paprika samples. *P Red* and *SY* correspond to Para Red-adulterated and Sunset Yellow-adulterated paprika samples, respectively.

The performances of the classification models (Table 9) indicate good sensitivity and excellent specificity.

Table 9: Discriminant analysis classification performances.

Model	**Class**	**Actual size**	**Predicted group (%)** *Sud*	*Non-Sud*	**Sensitivity %**	**Specificity %**
A	*Sud*	126	119 (94.4)	7 (5.6)	94.4	73.8
	Non-Sud	84	22 (26.2)	64 (73.8)		
Cross-validation						
	Sud	126	118 (93.7)	8 (6.3)	93.7	73.8
	Non-Sud	84	22 (26.2)	62 (73.8)		
			Sud	*PRed*	*SY*	
B	*Sud*	126	114 (90.5)	11 (8.7)	1 (0.8)	90. 86.9
	PRed	42	4 (9.5)	37 (88.1)	1 (2.4)	
	SY	42	5 (11.9)	0	37(88.1)	

Sud, Non-Sud correspond to Sudan dyes-adulterated and non-Sudan dye-adulterated paprika samples, respectively whereas *P Red* and *SY* correspond to Para Red-adulterated and Sunset Yellow-adulterated paprika samples, respectively.

The overall correct classifications of original samples were 86.2% and 89.5% for models A and B, respectively. Of particular interest was model A which classified the adulterated paprika samples into Sudan dye-adulterated and non-Sudan dye-adulterated paprika with a cross-validated correct classification of 85.7%. This indicates robustness of the method. It also confirms the adequacy of the WDXRF spectral features which are Compton and Rayleigh scatters as well as their derivative ratios, to differentiate between Sudan dyes-adulterated and non-Sudan dyes-adulterated paprika samples, as revealed by the logistic regression method. The overall correct classifications in the discriminant analysis model A increased by 3% compared with the logistic regression model. Additionally, the sensitivity and specificity were

significantly increased in the DA model A (Table 9) compared to the logistic regression analysis. There were similar misclassifications in the DA as was observed in the logistic regression classification. Some Sudan dyes-adulterated samples (Sud) were classified as Para Red and Sunset Yellow-adulterated (non-Sud) and vice versa. This was due to the structural relatedness of Sudan I dye with Para Red dye and vice versa. This was confirmed when the 'non-Sud' group was sub-divided into two of Para Red-adulterated (P Red) and Sunset Yellow-adulterated (SY) in model B. About 8.7% of Sudan dyes-adulterated samples (Sud) were classified as Para Red-adulterated (P Red), whereas 9.5% were classified vice versa. The discriminant analysis confirmed the ability of WDXRF to differentiate between Sudan dyes-adulterated and non-Sudan dye-adulterated paprika samples with high accuracy, as was already revealed by the logistic regression. The ability of WDXRF to accurately predict the type adulteration in paprika adulterated with and without Sudan dyes is of great importance in the use WDXRF to screen for illegal dyes such as the Sudan dyes in paprika. Further, this established ability also serves as a platform for the investigation of the ability of WDXRF to predict the levels of adulteration in paprika samples predicted (or suspected) to be adulterated with Sudan and non-Sudan dyes.

3.3 Multiple Regression Analysis

Three (3) multiple regression models were prepared for paprika and sweet pepper adulterated with each of the 5 dyes (Sudan I, Sudan III, Sudan IV, Para Red and Sunset Yellow FCF). Model *A* was based on the Compton and Rayleigh ratios, *B* based on the Compton and Rayleigh scatter intensities whereas model *C* was the full model based on all four spectral quantities (Compton and Rayleigh intensities and their derivative ratios). The best models were selected based on the goodness of fit (Adjusted R^2), Mallow's Cp statistic, Akaike Information Criterion (AIC) and the standard error of estimate (SEE) associated with the models. The variance inflation factors (VIFs) of the predictors in each model were also discussed. Table 10 summarizes adjusted R2, Akaike Information criterion and the standard errors of estimate of the fitted multiple regression models.

Table 10: Summary of performances of the three multiple regression models.

% Adulteration	Adj. R^2 (%)			AIC			SEE (%)		
	A	***B***	***C***	***A***	***B***	***C***	***A***	***B***	***C***
Sudan I in paprika	76.0	94.4	98.2	4.4	2.9	1.8	8.2	4.0	2.5
Sudan III "	68.7	91.6	95.1	4.6	3.3	2.9	9.4	4.9	3.7
Sudan IV "	79.2	89.0	97.1	4.2	3.6	2.3	7.7	5.6	2.8
Para Red "	53.6	88.8	97.1	5.0	3.6	2.3	11.5	5.6	2.8
Sunset Yellow "	90.1	98.7	99.0	3.5	1.4	1.3	5.3	1.9	1.7
Sudan I in sweet p.	81.0	95.6	98.1	4.1	3.5	1.4	7.2	3.5	2.3
Sudan IV "	79.1	93.3	98.4	4.2	3.1	1.8	7.7	4.4	2.3

AIC is the Akaike Information Criterion and ***SEE*** is the standard error of estimate. Models *A, B,* and *C* had coefficients of 3, 3, and 5, respectively and Mallow's Cp values of 3, 3, and 5, respectively.

The adjusted R^2 statistic indicates the percentage of the observed variability in the percentage of adulteration which is explained by the independent variables in the fitted model. It indicates the goodness of the fitting. The model based on only the Compton and Rayleigh ratios had adjusted R^2 values between 53.6% and 90.1% (Table 10). Para Red- and Sunset Yellow-spiked paprika had the lowest and highest goodness of fit values, respectively. Although there were appreciable degree of fitting for all dyes in paprika and sweet pepper (>50%), the goodness of fit values suggest that the Compton and Rayleigh ratios alone may not be the ideal variables to predict levels of adulteration of paprika and sweet pepper suspected to be adulterated with Sudan dyes. Additionally, the standard errors of estimate in the models based on only the Compton and Rayleigh ratios (model A) were higher (between 5.3 and 11.5%) than the other models.

The model based on the Compton and Rayleigh (model B) scatter intensities had goodness of fit between 88.8% and 98.7% with the errors of estimate between 1.9 and 5.6%. The lowest and highest fitting were observed for Para Red and Sunset Yellow-spiked paprika, respectively whereas the lowest error was observed for Sunset Yellow dye. This was consistent in all three models. However, the highest errors of estimate in the model based only the scatter intensities were observed for Para Red and Sudan III paprika adulterations. These observations in the errors of estimate in model B were consistent with the errors in model C (based on both intensities and ratios).

The full model had goodness of fit ranging from 95.1% to 99.0% with estimated error between 1.7 and 3.7%. The highest fitting and lowest error of estimate were observed

consistently for Sunset Yellow-spiked paprika. This could be mainly due to the fact that Sunset Yellow is a hydrophilic dye compared to the other highly hydrophobic dyes; hence the paprika-dye interaction was more appropriate, among other things such as sample preparation errors and instrumental errors.

Generally, it was observed that there were significant improvements in the goodness of fit and the standard errors in most of the adulterations from model A to C. Of particular interest was the prediction of the levels of Para-Red adulteration in the adulterated paprika samples by the three models (Table 10), where there was a significant increase of about 44% in the adjusted R^2 values between models A and C, with corresponding decrease in the standard error of estimate from 7.5% to 2.8%, respectively. Similarly, there were significant increases ranging from 17% to 22%, with the exception of Sunset Yellow adulterated paprika, in the fitting between models A and C, with corresponding decrease in the standard error of estimate between 8.6% and 3.6%.

There were minimal increases in the fitting of the model with corresponding decreases in the errors of estimate between paprika and sweet pepper adulterated with Sudan I and IV dyes. In other words, the models explained better, the observed variances in the Sudan I and IV-adulterated sweet pepper samples than in their corresponding paprika samples. This may be due the slight differences in the elemental compositions paprika and sweet pepper but how they cause about this is not clearly understood.

The Mallow's Cp statistic measures the bias in a multiple regression model by comparing the total mean squared error with the true variance. An unbiased model has an approximate Cp value of *p*, where *p* is the number of coefficients in the model (including the constant). The Mallow's Cp values for models A, B, and C were 3, 3, and 5, respectively, indicating that all three models were unbiased. The absence of bias in the models indicates that the prediction of the levels of adulteration by the models were accurate.

The Akaike Information Criterion (AIC) is based on the residual mean squared errors with a penalty that grows with increasing number of coefficients in the model. Depending on the selected information criterion, models with the smallest residual errors with as few coefficients as possible is desirable. The observed AICs (Table 10) ranged from 3.5 to 5.0, 1.4 to 3.6, and 1.3 to 2.9; for models based on the ratios (A), scatter intensities (B), and both ratios and scatter intensities (C), respectively. These

findings indicated that the penalties reduced from models based on the ratios to the full models based on both the ratios and scatter intensities.

3.3.1 Variance Inflation Factor (VIF)

The Variance Inflation Factor (VIF) in multiple regression analysis is an indicator of multicollinearity regression models and computationally reciprocates the tolerance of a regression model. It states the inflation in the magnitude of the standard errors associated with a particular beta weight due to multicollinearity. A maximum VIF of 10 was allowed in this study. Summary of the VIFs as well as the tolerance in the three models are shown in Table 2 below.

Table 11: VIFs and tolerances of the multiple regression models.

Adulteration	***Model A***	***Model B***	***Model C***			
			Comp rat.	Ray rat.	Rh Comp	Rh Ray
Sud I pap	4.98 (0.20)	1.06 (0.95)	18.30(0.06)	87.17(0.01)	3.95(0.25)	71.06(0.01)
Sud III "	3.36 (0.30)	1.40 (0.71)	27.75(0.04)	52.68(0.02)	11.72(0.09)	44.13(0.02)
Sud IV "	4.32 (0.23)	1.28 (0.78)	32.10(0.03)	56.01(0.02)	9.31(0.11)	18.27(0.06)
Para Red "	9.39 (0.11)	2.76 (0.36)	24.52(0.04)	50.49(0.02)	6.70(0.15)	23.82(0.04)
S Yellow "	10.13(0.10)	4.22 (0.24)	49.27(0.02)	92.39(0.01)	29.03(0.03)	50.46(0.02)
Sud I swt p	4.59(0.22)	1.10 (0.91)	20.42(0.05)	50.45(0.02)	5.07(0.20)	30.01(0.03)
Sud IV swt p	2.96 (0.34)	1.05 (0.95)	18.99(0.05)	172.15(0.01)	7.75(0.13)	134.41(0.01)

Sud I refer to Sudan I, *Sud III* and *Sud IV* refer to Sudan III and Sudan IV dyes. *Pap* and *Swt p.* refer to paprika and sweet pepper. *Model A* is model based on the Compton and Rayleigh ratios; *Model B*: based on Rh Compton and Rayleigh scatter intensities; and *Model C* is the full model based on both ratios and scatter intensities. *Comp rat, Ray rat, Rh Comp*, and *Rh Ray* refer to the Compton ratio, Rayleigh ratio, Rh Compton and Rayleigh scatter intensities, respectively. The unbracketed and bracketed figures are the VIFs and tolerances, respectively.

The VIFs for the models based on the scatter intensities (1.05-4.22) and ratios (2.96-10.1) were very low compared to the VIFs for the full model (C), indicating the presence of multicollinearity in the full model. However, the multicollinearity in the full model was expected as the Compton and Rayleigh ratios are derivatives of the Compton and Rayleigh scatter intensities, respectively, obtained by comparisons of the measured scatter intensities of the sample to the theoretical intensity if the simulated matrix. Besides, the ratios and intensities provide different spectral information from

the measured samples. The Compton and Rayleigh scatter intensities are based on physical characteristics of the measured samples whereas the ratios take into account the nature of the sample compared to the matrix the simulated matrix (cellulose).

Regarding this, the full models seem to be the best model. Additionally, since the standard errors of estimate and thus the variances in the full models are significantly less than in the model based on the Compton and Rayleigh scatter intensities, the inflation in the variances (VIFs) in the full model may not significantly affect the predictions of the levels of adulteration using the full model. Besides, since the Compton and Rayleigh scatter intensities as well as their derivative ratios are readily available in any WDXRF spectra, both models could be used for the prediction of levels of adulteration and the results compared with each other for any significant differences.

Based on the significantly higher goodness of fit values, coupled with significantly lower standard errors of estimate and information criterion penalties, it is concluded that the best model to predict the levels of adulteration in paprika and sweet pepper adulterated with Sudan (I, III, IV and Para Red) and Sunset Yellow FCF dyes is the full model based on the Compton and Rayleigh ratios with the Rh Compton and Rayleigh scatter intensities. In other words, the Compton and Rayleigh ratios together with the Rh Compton and Rayleigh scatter intensities are the best predictors of levels of adulteration in paprika and sweet pepper adulterated with Sudan and Sunset Yellow FCF dyes.

4. CONCLUSIONS

The ability of WDXRF to predict the types of adulteration of paprika and sweet pepper with Sudan I, III, IV, Para Red and Sunset Yellow dyes using logistic regression as well as discriminant analysis has been investigated. Additionally, the ability of WDXRF to predict the levels of adulteration of paprika and sweet pepper samples suspected of adulteration with the fore-mentioned dyes was also investigated.

The results obtained in this study shows that WDXRF coupled with multivariate analysis such as logistic regression and discriminant analysis can adequately predict the type of adulteration of paprika and sweet pepper adulterated with Sudan dyes and with Para Red or Sunset Yellow dyes with very high sensitivity and appreciable degree of specificity based on the Compton and Rayleigh scatter intensities and their derivative ratios which are natural components of WDXRF spectra.

Further, the results obtained in this study shows that WDXRF can effectively predict the levels of adulteration of paprika and sweet pepper detected or suspected to be adulterated with Sudan I, III, IV, Para Red, and Sunset Yellow dyes with very excellent degrees of accuracy and corresponding minimal errors. The full model is the best model to predict the levels of adulteration of paprika and sweet pepper samples adulterated with Sudan I, III, IV, Para Red, and Sunset Yellow FCF dyes and the best predictors are the natural WDXRF spectral features of Compton and Rayleigh scatter intensities with their derivative ratios as the predictors.

WDXRF seem to be a promising tool for screening of Sudan dyes in spices and can thus be an alternative for the analysis of Sudan dyes in spices.

5. RECOMMENDATIONS FOR FURTHER WORK

A comparative study of the performance of the developed models based on the WDXRF technique with standard methods such as HPLC will be appropriate for the validation of the developed WDXRF method to predict the levels of adulteration of paprika and sweet pepper with Sudan dyes.

It will be interesting to repeat the study focusing on lower adulteration levels, for example, between 0.1% to1% (w/w) (or lesser), with more replicates to evaluate the limits of the WDXRF technique to predict the types of dye adulteration as well as the levels of adulteration.

There were lots of spice samples such as curry, saffron, etc. which were not used in this study. The ability of the WDXRF technique to predict levels of adulteration in these spices and blends of spices as well as with blends of Sudan dyes will be worth researching given reports of simultaneous detection of Sudan I and IV dyes in some spices.

The application of the findings of this study to predict the type and levels of Sudan dyes adulteration in other foodstuffs such as edible oils will be worth investigating to add to the already known usefulness of WDXRF in the food industry.

6. REFERENCES

An, Y., Jiang, L., Cao, J., Geng, C., & Zhong, L. (2007). Sudan I induces genotoxic effects and oxidative DNA damage in HepG2 cells. *Mutation Research, 627*(2), 164–70. doi:10.1016/j.mrgentox.2006.11.004

Anfossi, L., Baggiani, C., Giovannoli, C., & Giraudi, G. (2009). Development of enzyme-linked immunosorbent assays for Sudan dyes in chilli powder, ketchup and egg yolk. *Food Additives & Contaminants. Part A, Chemistry, Analysis, Control, Exposure & Risk Assessment*, *26*(6), 800–807. doi:10.1080/02652030902755283

ASTA (American Spices Trade Association). (2005). *Sudan Red and Related Dyes – White Paper*. Retrieved from http://www.astaspice.org/food-safety/white-papers/

Au, W., & Hsu, T.C. (1979). Studies on the clastogenic effects of bilogic stains and dyes. *Environmental Mutagenesis,* 1, 27-35. doi:10.1002/em.2860010109

Bafana, A., Devi, S. S., & Chakrabarti, T. (2011). Azo dyes : past , present and the future. *Environmental Reviews,* 19, 350–370. doi:10.1139/A11-018

Bertin, E.P. (1978). Introduction to X-ray spectrometric analysis. Plenum Press, New York-London.

Bhattacharjee, M. (2014). Evaluation of mitodepressive effect of Sunset Yellow using Allium sativum assay, *3*(3), 1120–1130.

Brouwer, P. (2010). *Theory of XRF* (3rd ed.). Almelo, The Netherlands: PANalytical B.V. Amelo, The Netherlands.

Cameron, T.P., Hughes, T.J., Kirby, P.E., Fung, V.A., & Dunkel, V.C. (1987). Mutagenic activity of 27 dyes and related chemicals in the salmonella microsome and mouse Lymphoma TKþ assays. *Mutation Research,* 189, 223-261. doi:10.1016/0165-121(87)90056-5

Chen, H. (2006) Recent advances in azo dye degrading enzyme research. *Current Protein &Peptide Science,* 7, 101-111.

Chen, H., Feng J., Kweon, O., Xu H., & Cerniglia, C.E. (2010). Identification and molecular characterization of a novel flavin-free NADPH preferred azoreductase encoded by azoB in *Pigmentiphaga kullae* K24. *BMC Biochemistry*, 11:13. doi:10.1186/1471-2091-11-3

Chen, H., Hopper, S. L., & Cerniglia, C. E. (2005). Biochemical and molecular characterization of an azoreductase from Staphylococcus aureus, a tetrameric NADPH-dependent flavoprotein. *Microbiology (Reading, England)*, *151*(Pt 5), 1433–41. doi:10.1099/mic.0.27805-0

Chen, H., Wang, R.F., & Cerniglia, C.E. (2004). Molecular cloning, overexpression, purification, and characterization of an aerobic FMN-dependent azoreductase from Enterococcus faecalis. *Protein Expression and Purification*, 34, 302-310.

Chung, K.T., Stevens, Jr. S.E., & Cerniglia, C.E. (1992). The reduction of azo dyes by the intestinal microflora. *Critical Reviews in Microbiology*, 18, 175-190.

Collier, S.W., Storm, J.E., Bronaugh, R.L. (1993) Reduction of azo dyes during in vitro percutaneous absorption. *Toxicology and Applied Pharmacology*, 118:73-79.

Colour Index. (2001) Fourth Edition. Available at: http://www.colour-index.org/.

Commission Decision 2003/460/EC. Available at: http://europa.eu.int/eurlex/pri/en/oj/dat/2003/l_154/l_15420030621en01140115.pdf

Commission Decision 2004/92/EC Available at: http://europa.eu.int/eurlex/pri/en/oj/dat/2004/l_027/l_02720040130en00520054.pdf

Commision Decision (2009) Commission Decision 2009/669/EC. *Official Journal of European Commununity*, (669), 1–22.

Di Anibal, C., Rodriguez, M. S., & Albertengo, L. (2014). UV-Visible Spectroscopy and Multivariate Classification as a Screening Tool to Identify Adulteration of Culinary Spices with Sudan I and Blends of Sudan I + IV Dyes. *Food Analytical Methods*, *7*(5), 1090–1096. doi:10.1007/s12161-013-9717-2

Di Anibal, C. V, Marsal, L. F., Callao, M. P., & Ruisánchez, I. (2012). Surface Enhanced Raman Spectroscopy (SERS) and multivariate analysis as a screening tool for detecting Sudan I dye in culinary spices. *Spectrochimica Acta. Part A, Molecular and Biomolecular Spectroscopy*, *87*, 135–41. doi:10.1016/j.saa.2011.11.027

Di Anibal, C. V, Odena, M., Ruisánchez, I., & Callao, M. P. (2009). Determining the adulteration of spices with Sudan I-II-II-IV dyes by UV-visible spectroscopy and multivariate classification techniques. *Talanta*, *79*(3), 887–92. doi:10.1016/j.talanta.2009.05.023

Di Anibal, C. V., Ruisánchez, I., & Callao, M. P. (2011). High-resolution 1H Nuclear Magnetic Resonance spectrometry combined with chemometric treatment to identify adulteration of culinary spices with Sudan dyes. *Food Chemistry*, *124*(3), 1139–1145. doi:10.1016/j.foodchem.2010.07.025

Dixit, S., Mishra, K. K., Khanna, S. K., & Das, M. (2008). Bezoate and Synthetic Color Risk Assessment of Fast Food Sauces Served at Street Food Joints of Lucknow, India. *American Journal of Food Technology*, *3*(3), 183–191.

Dixit, S., Purshottam, S. K., Khanna, S. K., & Das, M. (2011). Usage pattern of synthetic food colours in different states of India and exposure assessment through commodities preferentially consumed by children. *Food Additives & Contaminants. Part A, Chemistry, Analysis, Control, Exposure & Risk Assessment*, *28*(8), 996–1005. doi:10.1080/19440049.2011.580011

Downham, A., & Collins, P. (2000). Colouring our foods in the last and next millennium. *International Journal of Food Science & Technology*, *35*(1), 5–22. doi:10.1046/j.1365-2621.2000.00373.x

EFSA Scientific Opinion. (2005). Opinion of the Scientific Panel on Food Additives , Flavourings , Processing Aids and Materials in Contact with Food on a request from the Commission to Review the toxicology of a number of dyes illegally present in food in the EU Question number EFSA-200. *The EFSA Journal*, 263, 1–71.

EFSA Scientific Opinion. (2009). Scientific Opinion on the re-evaluation of Sunset Yellow FCF (E 110) as a food additive. *The EFSA Journal*, *7*(11), 1330. doi:10.2903/j.efsa.2009.1330

Feng, J., Heinze, T.M., Xu, H., Cerniglia, C.E., & Chen, H. (2010). Evidence for significantly enhancing reduction of Azo dyes in Escherichia coli by expressed cytoplasmic Azoreductase (AzoA) of Enterococcus faecalis. *Protein and Peptide Letters,* 17, 578-584. doi:10.2174/092986610791112701

Fonovich, T. M. (2013). Sudan dyes: are they dangerous for human health? *Drug and Chemical Toxicology*, *36*(3), 343–52. doi:10.3109/01480545.2012.710626

FoodSafetyHelpline.com. Available at: http://foodsafetyhelpline.com/2014/01/spices-board-has-ordered-to-destroy-spices-contaminated-with-sudan-dyes-in-compliance-to-fss-act-2006/ (Accessed June 2014).

Garfield, S. (2002) Mauve: how one man invented a colour that changed the whole world. W.W. Norton & Company, NY.

Garner, R.C., & Nutman, C.A. (1977). Testing of some azo dyes and their reduction products for mutagenicity using Salmonella typhimurium TA 1538. *Mutation Research* 44(1), 9-19. doi:10.1016/0027-5107(77)90110-5

Ghosh, P. K., & Jayas, D. S. (2009). Use of spectroscopic data for automation in food processing industry. *Sensing and Instrumentation for Food Quality and Safety*, *3*(1), 3–11. doi:10.1007/s11694-008-9068-7

Gonçalves, L. M. L., Costa, I. M., & Brito, J. A. A. (2011). Assessment of metal elements in final drug products by wavelength dispersive X-ray fluorescence spectrometry. *Analytical Methods*, *3*(7), 1468. doi:10.1039/c1ay05133d

Hashem, M. M., Atta, A. H., Arbid, M. S., Nada, S. A, & Asaad, G. F. (2010). Immunological studies on Amaranth, Sunset Yellow and Curcumin as food colouring agents in albino rats. *Food and Chemical Toxicology : An International Journal Published for the British Industrial Biological Research Association*, *48*(6), 1581–6. doi:10.1016/j.fct.2010.03.028

Hondrogiannis, E., Peterson, K., Zapf, C. M., Roy, W., Blackney, B., & Dailey, K. (2012). The use of wavelength dispersive X-ray fluorescence and discriminant analysis in the identification of the elemental composition of cumin samples and the determination

of the country of origin. *Food Chemistry*, *135*(4), 2825–31. doi:10.1016/j.foodchem.2012.07.003

Hondrogiannis, E., Rotta, K., & Zapf, C. M. (2013). The use of wavelength dispersive X-ray fluorescence in the identification of the elemental composition of vanilla samples and the determination of the geographic origin by discriminant function analysis. *Journal of Food Science*, *78*(3), C395–401. doi:10.1111/1750-3841.12050

IARC (International Agency for Research on Cancer), Lyon. (1975). IARC monographs on the evaluation of the carcinogenic risk of chemicals to man: some aromatic azo compounds 8, 224–231.

Jenkins, R. (1974) An Introduction to X-Ray Spectrometry. Heyden, London – New York – Rheine.

Johnson, G. E., Quick, E. L., Parry, E. M., & Parry, J. M. (2010). Metabolic influences for mutation induction curves after exposure to Sudan-1 and para red. *Mutagenesis*, *25*(4), 327–33. doi:10.1093/mutage/geq009

Karoui, R., & Debaerdemaeker, J. (2007). A review of the analytical methods coupled with chemometric tools for the determination of the quality and identity of dairy products. *Food Chemistry*, *102*(3), 621–640. doi:10.1016/j.foodchem.2006.05.042

Kirk-Othmer. (2004). Kirth-Othmer Encyclopedia of Chemical Toxicology. Volume 17.

López, M. I., Trullols, E., Callao, M. P., & Ruisánchez, I. (2014). Multivariate screening in food adulteration: untargeted versus targeted modelling. *Food Chemistry*, *147*, 177–81. doi:10.1016/j.foodchem.2013.09.139

Mekkawy, H. A., Ali, M. O., & El-Zawahry, A.M. (1998). Toxic effect of synthetic and natural food dyes on renal and hepatic functions in rats *Toxicology Letters* (Supplement), 1, 155-165.

Mishra, K.K., Dixit, S., Purshottam, S.K., Pandey, R.C., Das, M., & Khanna, S.K. (2007). Exposure assessment to Sudan dyes through consumption of artificially coloured chilli powders in India. *International Journal of Food Science and Technology*. 42, 1363–1366.

Murrell, J.N. (1973). The theory of the electronic spectra of organic molecules. John Wiley & Sons, NJ.

Pan, H., Feng, J., He, G.-X., Cerniglia, C. E., & Chen, H. (2012). Evaluation of impact of exposure of Sudan azo dyes and their metabolites on human intestinal bacteria. *Anaerobe*, *18*(4), 445–53. doi:10.1016/j.anaerobe.2012.05.002

Perring, L., Andrey, D., Basic-Dvorzak, M., & Blanc, J. (2005). Rapid multimineral determination in infant cereal matrices using wavelength dispersive X-ray fluorescence. *Journal of Agricultural and Food Chemistry*, *53*(12), 4696–700. doi:10.1021/jf047895+

Poul, M., Jarry, G., Elhkim, M. O., & Poul, J.-M. (2009). Lack of genotoxic effect of food dyes amaranth, sunset yellow and tartrazine and their metabolites in the gut micronucleus assay in mice. *Food and Chemical Toxicology : An International Journal Published for the British Industrial Biological Research Association*, *47*(2), 443–8. doi:10.1016/j.fct.2008.11.034

Rafii, F., Hall, J.D., & Cerniglia, CE. (1997). Mutagenicity of azo dyes used in foods, drugs and cosmetics before and after reduction by Clostridium species from the human intestinal tract. *Food and Chemical Toxicology*, 35, 897-901.

Rao, P., & Sudershan, R.V. (2008). Risk assessment of synthetic colors: a case study in Hyderabad, India. *International Journal of Food Safety, Nutrition and Public Health* 1, 68–86.

RASFF (2005). Rapid Alert System for Food and Feed, Annual Report. Available at: http://ec.europa.eu/food/food/rapidalert/report2005_en.pdf (Accessed March 2014).

Rebane, R., Leito, I., Yurchenko, S., & Herodes, K. (2010). A review of analytical techniques for determination of Sudan I-IV dyes in food matrixes. *Journal of Chromatography. A*, *1217*(17), 2747–57. doi:10.1016/j.chroma.2010.02.038

Refat, N.A., Ibrahim, Z.S., Moustafa, G.G., Sakamoto, K.Q., Ishizuka, M., & Fujita, S. (2008). The induction of cytochrome P450 1A1 by Sudan dyes. *Journal of Biochemical and Molecular Toxicology*, 22(2), 77-84. doi:10.1002/jbt.20220

Stiborová, M., Dračínská, H., Martínek, V., Svášková, D., Hodek, P., Milichovský, J., … Frei, E. (2013). Induced expression of cytochrome P450 1A and NAD(P)H:quinone oxidoreductase determined at mRNA, protein, and enzyme activity levels in rats exposed to the carcinogenic azo dye 1-phenylazo-2-naphthol (Sudan I). *Chemical Research in Toxicology*, *26*(2), 290–9. doi:10.1021/tx3004533

Stiborová, M., Martínek, V., Rýdlová, H., Koblas, T., & Hodek, P. (2005). Expression of cytochrome P450 1A1 and its contribution to oxidation of a potential human carcinogen 1-phenylazo-2-naphthol (Sudan I) in human livers. *Cancer Letters*, *220*(2), 145–54. doi:10.1016/j.canlet.2004.07.036

Stiborová, M., Martínek, V., Rýdlová, H., Microsomes, L., & Stiborova, M. (2002). Sudan I Is a Potential Carcinogen for Humans : Evidence for Its Metabolic Activation and Detoxication by Human Recombinant Cytochrome P450 1A1 and Liver Microsomes Sudan I Is a Potential Carcinogen for Humans : Evidence for Its Metabolic Activation and De, 5678–5684.

Tanaka, T. (1996). Reproductive and neurobehavioral effects of Sunset yellow FCF administered to mice in the diet. *Toxicology and Industrial Health*, 12(1), 69-79.

Tripathi, M., Dixit, S., Khanna, S. K., & Das, M. (2010). Intake pattern of synthetic colours by different age and socio-economic consumer groups of Lucknow , India, *3*(1), 19–31.

Tripathi, M., Khanna, S.K., & Das, M. (2007). Surveillance on use of synthetic colours in eatables vis a vis Prevention of Food Adulteration Act of India. Food Control 18, 211–219.

Vitale, R., Bevilacqua, M., Bucci, R., Magrì, A. D., Magrì, A. L., & Marini, F. (2013). A rapid and non-invasive method for authenticating the origin of pistachio samples by NIR spectroscopy and chemometrics. *Chemometrics and Intelligent Laboratory Systems*, *121*, 90–99. doi:10.1016/j.chemolab.2012.11.019

Wang, Y., Wei, D., Yang, H., Yang, Y., Xing, W., Li, Y., & Deng, a. (2009). Development of a highly sensitive and specific monoclonal antibody-based enzyme-linked immunosorbent assay (ELISA) for detection of Sudan I in food samples. *Talanta*, *77*(5), 1783–1789. doi:10.1016/j.talanta.2008.10.016

Xing, Y., Meng, M., Xue, H., Zhang, T., Yin, Y., & Xi, R. (2012). Development of a polyclonal antibody-based enzyme-linked immunosorbent assay (ELISA) for detection of Sunset Yellow FCF in food samples. *Talanta*, *99*, 125–31. doi:10.1016/j.talanta.2012.05.029

Xu, H., Heinze, T. M., Chen, S., Cerniglia, C. E., & Chen, H. (2007). Anaerobic metabolism of 1-amino-2-naphthol-based azo dyes (Sudan dyes) by human intestinal microflora. *Applied and Environmental Microbiology*, *73*(23), 7759–62. doi:10.1128/AEM.01410-07

Xu, H., Heinze, T. M., Paine, D. D., Cerniglia, C. E., & Chen, H. (2010). Sudan azo dyes and Para Red degradation by prevalent bacteria of the human gastrointestinal tract. *Anaerobe*, *16*(2), 114–9. doi:10.1016/j.anaerobe.2009.06.007

Yadav, A., Kumar, A., Tripathi, A., & Das, M. (2013). Sunset yellow FCF, a permitted food dye, alters functional responses of splenocytes at non-cytotoxic dose. *Toxicology Letters*, *217*(3), 197–204. doi:10.1016/j.toxlet.2012.12.016

Yellepeddi, R., & Thomas, R. (2006). New Developments in Wavelength-Dispersive XRF and XRD for the Analysis of Foodstuffs and Pharmaceutical Materials, *21*(September), 36–41.

Yu, L., Mao, Y., Gao, Y., & Qu, L. (2013). Sensitive and Simple Voltammetric Detection of Sudan I by Using Platinum Nanoparticle-Modified Glassy Carbon Electrode in Food Samples. *Food Analytical Methods*, *7*(6), 1179–1185. doi:10.1007/s12161-013-9731-4

Zanoni, T. B., Lizier, T. M., Assis, M. D. D., Zanoni, M. V. B., & de Oliveira, D. P. (2013). CYP-450 isoenzymes catalyze the generation of hazardous aromatic amines after reaction with the azo dye Sudan III. *Food and Chemical Toxicology : An International Journal Published for the British Industrial Biological Research Association*, *57*, 217–26. doi:10.1016/j.fct.2013.03.035

Zeiger, E., Anderson, B., Haworth, S., Lawlor, T., & Mortelmans, K. (1988). Salmonella mutagenicity tests: IV. Results from the testing of 300 chemicals. *Environmental and Molecular Mutagenesis,* 11(Suppl. 12), 1-157.

Zhang, Q., Liu, C., Sun, Z., Hu, X., Shen, Q., & Wu, J. (2012). Authentication of edible vegetable oils adulterated with used frying oil by Fourier Transform Infrared Spectroscopy. *Food Chemistry*, *132*(3), 1607–1613. doi:10.1016/j.foodchem.2011.11.129

7. APPENDIX

7.1 Pictures of WDXRF analyser, adulterated spices in sample cups and steel cup holders.

Figure 14: Bruker S4 Pioneer Commercial WDXRF Spectrometer used for the study.

Figure 15: Prepared spice samples in sample cups and steel sample cup holders (left). Sample cups containing spices adulterated with different dyes (right).